

4

~~DTIC FILE COPY~~

AFAL-TR-88-050

AD:



Final Report
for the period
1 May 1983 to
30 September 1987

High-Speed Laser Photography

August 1988

Author:
R. J. Becker

University of Dayton
Research Institute
300 College Park
Dayton, Ohio 45469-0001

AD-A202 293

UD-TR-88-45
F04611-83-K-0023
F04611-86-K-0018

Approved for Public Release

Distribution is unlimited. The AFAL Technical Services Office has reviewed this report, and it is releasable to the National Technical Information Service, where it will be available to the general public, including foreign nationals.

DTIC
ELECTE
NOV 28 1988
S H D

Prepared for the:

Air Force
Astronautics
Laboratory

Air Force Space Technology Center
Space Division, Air Force Systems Command
Edwards Air Force Base,
California 93523-5000

DISTRIBUTION STATEMENT A

Approved for public release;
Distribution Unlimited

NOTICE

When U.S. Government drawings, specifications, or other data are used for any purpose other than a definitely related Government procurement operation, the fact that the Government may have formulated, furnished, or in any way supplied the said drawings, specifications, or other data, is not to be regarded by implication or otherwise, or in any way licensing the holder or any other person or corporation, or conveying any rights or permission to manufacture, use, or sell any patented invention that may be related thereto.

FOREWORD

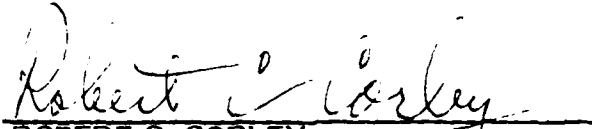
This final report was submitted by the University of Dayton Research Institute on completion of contract F04611-86-K-0018 with the Air Force Astronautics Laboratory (AFAL), Edwards AFB, CA. AFAL Project Manager was Gary Vogt.

This report has been reviewed and is approved for release and distribution in accordance with the distribution statement on the cover and on the DD Form 1473.


GARY L. VOGT
Project Manager


LAWRENCE P. QUINN
Chief, Aerothermochemistry Branch

FOR THE COMMANDER


ROBERT C. CORLEY
Deputy Chief, Astronautical Sciences
Division

Unclassified

SECURITY CLASSIFICATION OF THIS PAGE

REPORT DOCUMENTATION PAGE

1a. REPORT SECURITY CLASSIFICATION Unclassified		1b. RESTRICTIVE MARKINGS	
2a. SECURITY CLASSIFICATION AUTHORITY		3. DISTRIBUTION/AVAILABILITY OF REPORT Approved for public release, distribution unlimited.	
2b. DECLASSIFICATION/DOWNGRADING SCHEDULE			
4. PERFORMING ORGANIZATION REPORT NUMBER(S) UD-TR-88-45		5. MONITORING ORGANIZATION REPORT NUMBER(S) AFAL-TR-88-050	
6a. NAME OF PERFORMING ORGANIZATION University of Dayton Research Institute	6b. OFFICE SYMBOL (If applicable)	7a. NAME OF MONITORING ORGANIZATION Air Force Astronautics Laboratory	
6c. ADDRESS (City, State and ZIP Code) 300 College Park Dayton, OH 45469-0001		7b. ADDRESS (City, State and ZIP Code) YSCF Edwards Air Force Base, CA 93523-5000	
8a. NAME OF FUNDING/SPONSORING ORGANIZATION	8b. OFFICE SYMBOL (If applicable)	9. PROCUREMENT INSTRUMENT IDENTIFICATION NUMBER F04611-86-K-0018	
8c. ADDRESS (City, State and ZIP Code)		10. SOURCE OF FUNDING NOS.	
		PROGRAM ELEMENT NO.	PROJECT NO.
		TASK NO.	WORK UNIT NO.
11. TITLE (Include Security Classification) High-Speed Laser Photography (U)		62302F	5730
		00	PX
12. PERSONAL AUTHOR(S) Becker, Roger J.			
13a. TYPE OF REPORT Final	13b. TIME COVERED FROM 83/5/1 TO 87/9/30	14. DATE OF REPORT (Yr., Mo., Day) 88/8	15. PAGE COUNT 84
16. SUPPLEMENTARY NOTATION			
17. COSATI CODES		18. SUBJECT TERMS (Continue on reverse if necessary and identify by block number)	
FIELD	GROUP	cinephography	
21	08	solid propellants	
		laser photography	
		combustion	
19. ABSTRACT (Continue on reverse if necessary and identify by block number)			
<p>High-speed movies of solid propellant deflagration have long provided useful qualitative information on propellant behavior. Consequently, an extension of performance to include quantitative behavior of the surface, particularly the spacial relationship of particles across the surface, the temporal behavior of particles through extended periods of time, and accurate measurements of particle sizes, is highly desirable. Such measurements require the ability to take detailed movies across an extensive surface through the propellant flame for longer periods than the residence time of a given particle. For such experiments, camera optics employing magnification are undesirable, since they severely limit both the field of view and the depth of field, and hence, the useful duration of a frame sequence. Unfortunately, high resolution with magnification pushes both the diffraction limits and the performance capabilities</p> <p>(see reverse side)</p>			
20. DISTRIBUTION/AVAILABILITY OF ABSTRACT UNCLASSIFIED/UNLIMITED <input checked="" type="checkbox"/> SAME AS RPT. <input type="checkbox"/> DTIC USERS <input type="checkbox"/>		21. ABSTRACT SECURITY CLASSIFICATION Unclassified	
22a. NAME OF RESPONSIBLE INDIVIDUAL Gary L. Vogt		22b. TELEPHONE NUMBER (Include Area Code) (805) 375-5258	22c. OFFICE SYMBOL YSCF

Box 19 (Continued)

of standard lenses. At this limit, the modulation transfer function (MTF) of the camera optics and film will greatly affect performance. The MTF of the optics can be improved by a factor of two or more at practical spatial frequencies by the use of monochromatic light, such as the reflected light from a laser. This is especially true of off-axis rays, an important consideration when an extended field of view is required. The use of an intense, short-pulsed laser has the additional advantage of suppressing flame brightness and motion blur. Such a light source must retain a high repetition rate to follow temporal behavior in detail.

High resolution at unity magnification is achieved by the use of 2 mJ of illumination energy per pulse in conjunction with a fine-grain film. This approach has worked well on both aluminized and pure aluminum perchlorate propellants. Since the pulses provide enough light to expose fine-grain film at unity magnification, it is possible to encompass an entire 1/4-inch strand surface in our field of view. Motion blur at 7 kHz framing rates and unity magnification is negligible (1 μm) due to the 25 ns width of the laser pulses. The short pulse width is also helpful in circumventing flame turbulence.

The surfaces of the wide-distribution propellants were found to be molten. The intermediate-sized (20 microns) particles oscillate spontaneously on the surface following ignition. Ripples are seen on the surfaces of the large (400 microns) particles. A thin layer of smoke hugs the surface of the propellant.

The quantitative analysis of the data provided by a photograph of an entire 6-mm-x-9-mm strand surface, containing from 1×10^4 to 1×10^6 pixels, is a demanding task. Economical results of satisfactory accuracy can be obtained using optical data processing. Preliminary conclusions from movies made using a copper-vapor laser as a light source and an optical correlator are presented. Movies were taken across the burning surfaces of 1/4-inch strands cut at oblique angles with resolutions of 155 microns for periods of 0.2-0.5 seconds. The optical correlator has worked well in providing temporal and spatial correlations. Attainment of quantitative statistical data using this correlator requires full-field information of the type obtained in the reported movies.

Accession For	
NTIS GRA&I	<input checked="" type="checkbox"/>
DTIC TAB	<input type="checkbox"/>
Unannounced	<input type="checkbox"/>
Justification	
By	
Distribution/	
Availability Codes	
Dist	Avail and/or Special
A-1	

Keywords: Solid Propellant Rocket Engines, Solid Rocket Propellants, Combustion Chambers, Propellant Grain, Combustion, Cinephotography. (R6)



TABLE OF CONTENTS

<u>SECTION</u>	<u>PAGE NO.</u>
INTRODUCTION	1
Air Force Needs	1
Limitations of Conventional Techniques	2
Perspective	3
Scope	7
EXPERIMENTAL DISCUSSION	9
Hardware	9
Optical System	13
Degradation Due to Flame Turbulence	19
Physical Limits	13
Optics	20
Servopositioning Circuit	21
Opto-Mechanical Subsystems	22
Control Circuitry	26
Servoperformance	29
Local Burning Rate	30
Laser Development and Synchronization	
Electronics	32
Pulse Synchronization Circuit	32
Copper-Vapor Laser Development	34
Ancillary Work	36
Film Processing	36
Inhibitor Development	37
Optical Correlator	40
Concept	42
Practical Considerations and Limitations	44
Stereo Cinephotography	46
RESULTS	55
General Performance	55
AP Matrix Behavior	56
Deflagration Behavior	57
Correlator Results	62
Additional Observations	66
CONCLUSIONS	69
REFERENCES	71

LIST OF ILLUSTRATIONS

<u>FIGURE</u>		<u>PAGE NO.</u>
1	Reduction of Film Exposure From Flame by Use of a Line Filter.	4
2	Cross Section of Window Bomb.	9
3	Top View of Window Bomb.	10
4	Reentrant Window Port.	11
5	Modulation Transfer Function of Typical Single-Element Lens.	15
6	Modulation Transfer Function (MTF) of Film.	17
7	Modulation Transfer Function of White Light vs. Monochromatic Light.	17
8	Modulation Transfer Function vs. Field-of-View.	18
9	Coherence Spoiler.	21
10	Servooptics.	22
11	Mechanical Drive for Positional Controller.	23
12	Diode-Array Control Circuit.	25
13	Detector and Analog Conditioning Circuit.	26
14	Digital Processing Circuit.	27
15	Analog Control Circuit.	27
16	Eight-Element Circuit Prototype.	29
17	Photodiode Array Trace Showing Surface Location vs. Time.	32
18	Pulse Synchronization Block Diagram.	33
19	Qualitative Performance of Commonly Used Inhibitors for Strand Experiments.	38

LIST OF ILLUSTRATIONS
(Continued)

<u>FIGURE</u>		<u>PAGE NO.</u>
20	Chemical Structure of Phenolic Resin Copolymer Unit.	39
21	Qualitative Behavior of Polymer Inhibitor vs. Solution concentration.	41
22	Optical Correlator.	44
23	Untreated Photograph of Combusting Surface.	45
24	Correlation Function Obtained from Untreated Photograph.	46
25	High-Contrast Photograph of Combusting Surface.	47
26	Correlation Function Obtained From a High-Contrast Photograph.	48
27	Stereo Optics.	50
28	Side View of Window Bomb.	50
29	Stereo Images of Burning Propellant Surface.	51
30	Stereo Images of Burning Propellant Surface.	52
31	Stereo Images of Same Subject as Shown in Figure 29, Taken Several Frames Later.	53
32	Best Fit to Correlation-Width Data.	60
33	Exponential Fit to Size vs. Pressure Data.	64
34	Quadratic Fit to Size vs. Pressure Data.	65
35	Time Dependence of Correlation Peak Height.	66
36	Width of Cross-Correlation Functions vs. Separation in Time.	67

NOMENCLATURE

A	Adjustable parameter
b	Resolution of camera optics
b_1	Adjustable parameter
b_2	Adjustable parameter
B	Adjustable parameter
C	Adjustable parameter
D	Diameter of Camera lens
f	Focal length of camera lens
f#	f-number = f/D
$f(t)$	Functional form of theoretical curve fitting measured correlation peak heights versus time
$f(p)$	Functional form of theoretical curve for correlation width versus pressure
$f(x,y)$	Transmittance of first image
$h(x,y)$	Transmittance of second image
I	Signal intensity
k_c	Cut-off spatial frequency of camera optics
k_1	Effective cut-off spatial frequency
m	Intensity modulation of an image
m_1	Adjustable parameter
m_2	Adjustable parameter
M	Magnification of camera optics
p	Pressure
x	Horizontal image coordinate
x_0	Amount of translation of an image in the x direction
y	Vertical image coordinate

NOMENCLATURE
(Continued)

t	Time
z	Depth-of-field of camera optics
λ	Wavelength of laser light
ξ	Diffraction-limited resolution
ξ_T	Transverse resolution of cinephotographic system
ξ_d	Depth resolution
ω	Oscillation frequency
ν	Damping rate for oscillations
ϕ	Angle between two viewing perspectives

INTRODUCTION

AIR FORCE NEEDS

Both motor design and propellant design are abetted by detailed in-situ information on the deflagration behavior of propellant surfaces. Present understanding of the details of propellant combustion is sparse and would benefit from more detailed qualitative information, as well as quantitative information. (Ref. 1,2) More must be learned about localized, transient burning rates, their dependence on grain and binder composition and grain size distribution, and the coupling of regression rates of the various constituents in the grain. Solid propellants have a granular, heterogeneous composition. (Ref. 3) Consequently, local variations in their transient burning rates are expected. In fact, a spiked behavior in the local burning rate is known to occur in many propellants. If local transients couple to the acoustic field in the combustion chamber, the burning rate may oscillate, driving instabilities in the chamber. (Ref. 4-10) Detailed information on transient regression rates is poor. The provision of such data would be of great benefit both in propellant formulation and in motor design. The length scales of the heterogeneities range from 2 to 10^3 μm (the smallest being additives, the largest being oxidizers). Therefore, it has been anticipated that the phenomena pertaining to the combustion process of solid propellant possesses these length scales.

An experiment which provided clarity and detail for quantitative statistical analysis would be of tremendous help to the modelers. This type of information is available in high-speed movies of flows and combusting systems. Because of its high pixel density, a photograph has great advantages for recording topographic information. Solid propellant combustion is a prime example of a system for which detailed movies can provide much-needed information. To follow both the local and transient propellant response requires movies that simultaneously offer good spatial resolution and high framing rates. It is suspected that the combustion of individual particles is affected by their environment, possibly including other particles over regions that are quite large compared to individual particle dimensions. Moreover, the flame temperature and gas dynamics may not be properly representative of motor conditions if the cross section of a propellant test strand is too small, so it is desirable to obtain information over a wide field-of-view. Since it would also be helpful to observe the fully combusting surface for a time longer than the time it takes the largest particles in a given formulation to be completely consumed, movies should be made over extended time periods.

Much of these quantitative data could be organized in terms of correlation functions and probability density functions. This would require the automatic processing and analysis of a large

number of frame sequences. It would also require high-quality films of excellent resolution and a thorough characterization of the propellants and the burn conditions.

Many propellants are worthy of detailed photographic studies, but one class of special importance lacks the high-pressure exponents typical of conventional grains. Studies by Dr. R. Richard Miller of United Technologies Corp./Chemical Systems Division (CSD) show that these formulations exhibit an anomalous burning behavior as a function of grain size mix, (Ref. 11) which is not predicted by theory and is not well understood. The burning rate is extremely sensitive to the binding agent; changes in the burning rate by a factor of eight, due to the binder, have been observed. Miller found that the burning rate of the larger (400 μm) crystals follows a distinct, step-wise pattern. In many cases these grains undergo such strong changes in burning rates as to self-extinguish. Information similar to that found by Miller is needed on grains of smaller (20 μm) size.

A second important class of propellants uses aluminum as a fuel and ammonium perchlorate (AP) as an oxidizer. These formulations have a very high specific impulse but have been difficult to study, due to the opacity and luminosity of their flames. It is known that the heterogeneity of composition and grain size play an important role in their combustion, but the details of the effect of the interactions between the constitutive particles on the respective grain regression rates are not well known.

For the above reasons, the bulk of the experiments were run on wide-distribution AP propellants, with a few additional movies made on aluminized propellants. The emphasis in the program was to deliver to AFAL a data base on the microscopic and transient combustion of propellants which can be used in models of propellant combustion.

LIMITATIONS OF CONVENTIONAL TECHNIQUES

Presently, one means of obtaining the transient propellant burning rate is by the phase shift in a microwave cavity. (Ref. 12,13) The data acquired using the technique are impressive. However, it yields only an average oscillatory burning rate taken over the entire burning surface of the propellant. This technique is best suited for recording repetitive, sinusoidal oscillations; it is insensitive to secular transients. Finally, it is restricted to information about the regression rate of the strand itself. It gives no information about coupling to perturbations in the gas-phase combustion zone and would not readily be extended to geometries other than end-burning strands. To date, it has only been demonstrated successfully in burns occurring inside the waveguides. The applicability of such data to environments more closely approximating practical motors is not clear. Indeed, a Hilbert

transform analysis of microwave data has been made, showing that these data are very inaccurate.

Additional information has been obtained from a post-mortem analysis of the surfaces of quenched propellants. (Ref. 11,14-17) Much of the detailed understanding of segregation and sintering in mixed grain formations is based on such work. Unfortunately, it is not known to what extent the grain surface is altered during the quenching process.

Much of the present knowledge of propellant deflagration has been garnered by high-speed photography. (Ref. 18-20) However, cinephotography using conventional light sources is unable to resolve the burning particles hidden inside of their bright flames. Conventional cinephotography suffers from an inherent blur limitation, given by long ($10 \mu\text{s}$) shutter time. In addition, standard window bombs do little to isolate various aspects of the chamber environment, such as the magnitude and direction of the flow relative to the propellant surface. Such movies are made with white light, with effective shutter times on the order of a microsecond. These conditions would require film motion blur of seven microns for every increment of a thousand frames per second in the film framing rate at unity magnification. In fact, these movies are usually taken with an effective shutter time equal to a given fraction of the framing rate, with a "1/100th shutter" being about state of the art. This would result in 70-micron motion blur at unity magnification.

Most conventional films are taken at framing rates of 2000 to 4000 frames per second, with the bulk of them at the lower end of that range. This would limit their ability to follow one kilohertz oscillations in detail. Conventional movies obtain their peak resolution on the order of 25 microns ($15 \mu\text{m}$ has been claimed) through magnification. Magnification has the advantage of overcoming the blur problem due to the long shutter times in these movies. It also enables the experimenter to use large-grain film which does not require extremely intense light for exposure. However, every factor-of-two increase in magnification reduces the depth-of-field by a factor of four. Consequently, these movies must suffer not only from a reduced field-of-view due to their magnification, but also from a very limited depth-of-field. Since these movies are run without a servopositioner, this also limits the number of frames in focus within a sequence.

PERSPECTIVE

The objectives of the high-speed laser photography experiment are to develop an enhanced experimental capability of achieving high-resolution movies of propellant combustion over a wide field-of-view and an extended time period. The primary aim has been to obtain qualitative information, but demonstration of the potential of such films for providing quantitative data was

also sought. The approach taken has been to assemble a photographic system based upon a copper-vapor laser and a window bomb with wide optical access.

The use of an intense pulsed 510 nm laser for illumination relaxes some of the constraints germane to white-light illumination. Consequently, it is now possible to survey an entire strand surface in detail. In this manner, meaningful statistical information can be obtained about detailed particle behavior in the flame. In particular, analyses of interactions between particles and cooperative behavior, if any, may be made.

The initial concept for the experiments is due to Dr. Robert Glick. Single shots of burning propellant strands taken at UDRI with a YAG laser had demonstrated that a short, intense laser pulse is a perfect source of illumination for combustion photography. The energy of a large (1-2 mJ) laser pulse, restricted to a narrow bandwidth, is so much brighter than the hottest flame that when combined with appropriate camera filters, it can expose a film which shows little or no exposure from the flame. Hence, intense laser illumination serves to overwhelm flame brightness, allowing an unobscured view of the propellant surface. This property is abetted by the use of a line filter in the camera optics (Figure 1) and high resolution (160 line pairs/mm) film. An entire 6-mm-x-9-mm area can be photographed

- 1.4 mJ ILLUMINATION EXPOSES FINE-GRAIN FILM OVER ENTIRE FIELD OF VIEW
- FILTERING AND INTENSE MONOCHROMATIC LIGHT PULSE OVERCOME FLAME BRIGHTNESS

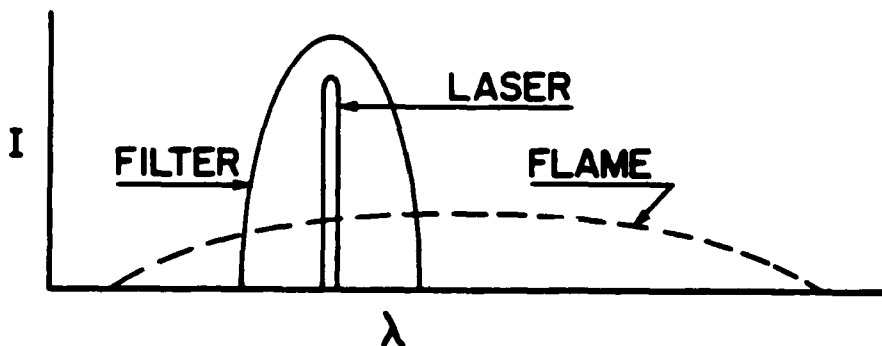


Figure 1. Reduction of Film Exposure From Flame by the Use of a Line Filter. This procedure is made possible by the use of monochromatic (laser) light.

with 15 micron resolution at unity magnification. Indeed, the laser illumination is so bright that a pulsed laser acts as a shutter--no mechanical shutter is required. The energy from the laser pulse is greater than the total flame emission integrated over the time between frames (200 μ s). This means that the effective shutter time is equal to the pulse width of the laser, which was 25 ns in the experiments described below. This is a factor of more than 40 better than that achieved using a flash lamp, and results in a motion blur of only one micron at a framing rate of 7,000 frames per second. In other words, the short width of the laser pulse freezes the motion of the object field, essentially eliminating motion blur.

The elimination of flame brightness and motion blur can be achieved in a film which shows a large (50 mm²) surface area. This suggests the possibility of studying the relationship of propellant behavior at one location to that of another location. This feature was noted by Dr. Miller and led to the major impetus for the experiments which were undertaken. However, since actual propellant behavior is of interest, combustion experiments using laser photography must provide rapid sequences of photographs--high-speed movies. The YAG laser is thus unsuitable as it has a typical repetition rate of 10 to 100 Hz. Glick's concept was to use the newly developed copper-vapor laser as a strobe source, since it has a repetition rate of several kHz. In the experiments undertaken, movies were made at framing rates of 6 to 7 kHz with laser energies of 1 to 2 mJ/pulse. Since copper-vapor lasers were still in an early developmental phase during the course of the program, a major challenge of the program was to marry the use of a copper-vapor laser to combustion cinephotography.

Conventional cinephotography of propellant combustion has been tried in two types of experiments. In the first type, attempts have been made to look at burning surfaces directly through flames. This type of experiment has not been very successful. In particular, it has been difficult to discern much of anything from stills of these movies; it has usually been necessary to have the eye effect an averaging of several frames while a movie was run. A typical spatial resolution for this type of experiment is 70 to 90 microns. Visual clarity has been greatly improved by photographing the progression of a flame front down the side of one-eighth inch strands. This type of experiment has been perfected at the Naval Weapons Center and has produced many spectacular movies. However, information about propellant behavior over large surface areas that are fully within a flame has been limited using this strategy.

The challenge in this program was to obtain useful visual clarity over surface areas of 40 mm² or more within a deflagrating region. This inherently raises difficulties with smoke and flame turbulence. In general, smoke was not a serious problem in the form that it is usually associated with, i.e.,

long plumes of smoke which obscure the view at distances of 1-3 cm from the surface. Although tufts of smoke did occur from localized regions of the surface, the vicinity of the surface was usually accessible. This was in part due to the use of a large (700 cubic inch) combustion bomb and a continuous purge of nitrogen. Good stills were routinely achieved with a resolution of 15 microns. However, the surface in the interior of the flame became increasingly indistinct as the operating pressure was increased. This was a serious problem at pressures of 400 psi. The highest operating pressure attempted was 650 psi. Most of the fuzziness of the pictures is due to flame turbulence.

The contrast and attendant resolution of a picture drop off extremely rapidly as random fluctuations in the optical path increase. In fact, the fall off goes exponentially with the square of the mean displacement of the optical path. Since a propellant flame inherently produces intense localized heating, the thermal gradients in the flame and the gas surrounding it are horrendous. These thermal gradients produce severe distortions in the optical path of any light passing through them, as well as severe phase shifts. The result is that flame turbulence acutely degrades both contrast and resolution, making it impossible to obtain good visual clarity and discern fine features. This problem will increase rapidly with flame temperature as well as operating pressure. A second difficulty is with a blanket of smoke confined to the immediate (100 to 500 μm) vicinity of the surface. Thus, a blanket of smoke lies over the surface and becomes increasingly dense as the operating pressure and the flame temperature increase. The smoke probably originates from the binder and apparently oxidizes by the time it leaves the surface region.

The most important finding of the program is that the surface in the interior of the flame is completely different in character from the surface adjacent to the flame. Immediately upon ignition, the surface becomes wet, and the sharp, angular features found exterior to the flame vanish completely. Although the large AP particles retain their individual identity, they are evidently very soft, since they undergo pronounced surface oscillations. They give the appearance of vibrating droplets. These oscillations always occur and can be discerned by the glint of the laser beam from the portion of the surface which is appropriately oriented with respect to the laser/camera optical system. As the surface contour of the large particles oscillate, the location of the bright spots move. As the operating pressure increases, the size of the bright areas increases, indicating that the soft AP particles are compressed toward the surface and have a flattened profile. The frequency of the oscillations also increases. At 400 psi, the frequency exceeds the 6 kHz repetition rate of the laser. This means that successive frames appear substantially different; therefore, rather than averaging several successive frames, the eye becomes confused.

The above features strongly suggest that experiments in which the leading edge of a propellant flame are observed may be misleading. In particular, it is inappropriate to attempt to improve the resolution of the movies in an effort to capture details of NWC-type films which are irretrievably lost due to flame turbulence and which are probably not even present in the flame interior. The present 15-micron resolution obtained in the absence of strong flame turbulence should be sacrificed for a greater depth of field.

If successful movies are possible at all at pressures over 800 psi, probably the only way they can be achieved is to use binders which do not smoke, or to make movies of ignition or possibly of flame quenching. Flame turbulence presents a fundamental difficulty that will limit high (25 micron) resolution movies to pressures below 400 psi. Resolution must be sacrificed if movies are made at higher operating pressures.

SCOPE

The program consisted of several tasks divided into three groups. The first group involved the setup of the experiment. This included construction of a windowed combustor optimized for the experiments, checkout of a state-of-the-art copper-vapor laser, implementation of a circuit for synchronizing the laser pulses with the camera framing rate, and development of a detailed experimental plan. The second set of tasks comprised the main focus of the proposed work--delivery of a data matrix on a sequence of selected propellants. The major goal of these experiments was to provide high-quality front-lit movies of improved resolution that enhanced our qualitative understanding of propellant deflagration. The third group of tasks consisted of attempts to extend our capability, using variants of our principal experimental technique, especially stereo cinephotography.

A customized windowed combustor was built for these experiments. The combustor was provided with a wide-angle window configuration optimized for stereo photographs of the strand surface. The combustor was TIG-welded from stainless steel tubing and commercial flanges. Circuitry to synchronize the laser pulses with the camera framing rate was designed and installed. A servopositioning circuit to maintain the strand surface within the depth-of-field of the camera optics was also designed and fabricated.

The main work consisted of front-lit profile studies of localized regression rates of a series of related propellant strands and their analysis. In the beginning, a matrix suggested by Richard Miller was used. The formulations were of ammonium perchlorate (AP) grains using IPDI and DDI curatives. Ten percent of the grain mix consisted of 20- μ m particles. Two-thirds of the mix consisted of 400- μ m and 2- μ m particles in a

five-part series of respectively 38/39, 41/36, 44/33, 47/30, and 50/27 percent. The remaining 13 percent of the formulation consisted of binder. Operating pressures were from 15 to 465 psi.

In addition to the matrix movies, front-lit high-speed stereo movies were also made of the burning surfaces of solid propellant strands at operating pressures up to 350 psi. Movies were made at viewing angles separated by 90 degrees to achieve a high depth resolution. These movies, which were recorded through flames across a 1/4 in. field-of-view, have a resolution of 25 μm . The stereo images were simultaneously recorded side by side on the same 16-mm frame by using X2 demagnifying optics and a mirror arrangement. The two images then passed through a single camera lens. Because of the complexity in the acquisition and reduction of stereo data, quantitative data analysis of stereo movies was attempted. This effort was undertaken solely to demonstrate feasibility and to provide qualitative information.

In summary, pulsed-laser cinephotography has eliminated problems with motion blur and flame brightness. Difficulties with a low-contrast object field have been met by a careful design of the camera optics. Laser speckle is not a problem. The experiments demonstrate that the surface of a deflagrating propellant is fundamentally different in the interior of the flame from the exterior at the flame edge. Flame turbulence wipes out detail in a film at pressures over a few hundred psi. Thus, pulsed-laser cinephotography is an excellent tool for studying physical processes inside a flame at low pressures, but cinephotography itself cannot access the interior of a flame with significant resolution at pressures above, approximately 800 psi.

EXPERIMENTAL DISCUSSION

This section describes the experimental apparatus and procedures. Approaches to various experimental problems are also discussed, as are the specifics of those problems. The first four paragraphs cover hardware, optics, and electronics. Minor efforts to support the photography program and a description of the photography experiments are given in the remainder of the section.

HARDWARE

A versatile seven-port window bomb was constructed with provisions for ease of maintenance and plentiful optical access (Figures 2 and 3). (Ref. 21) High-resolution movies demand

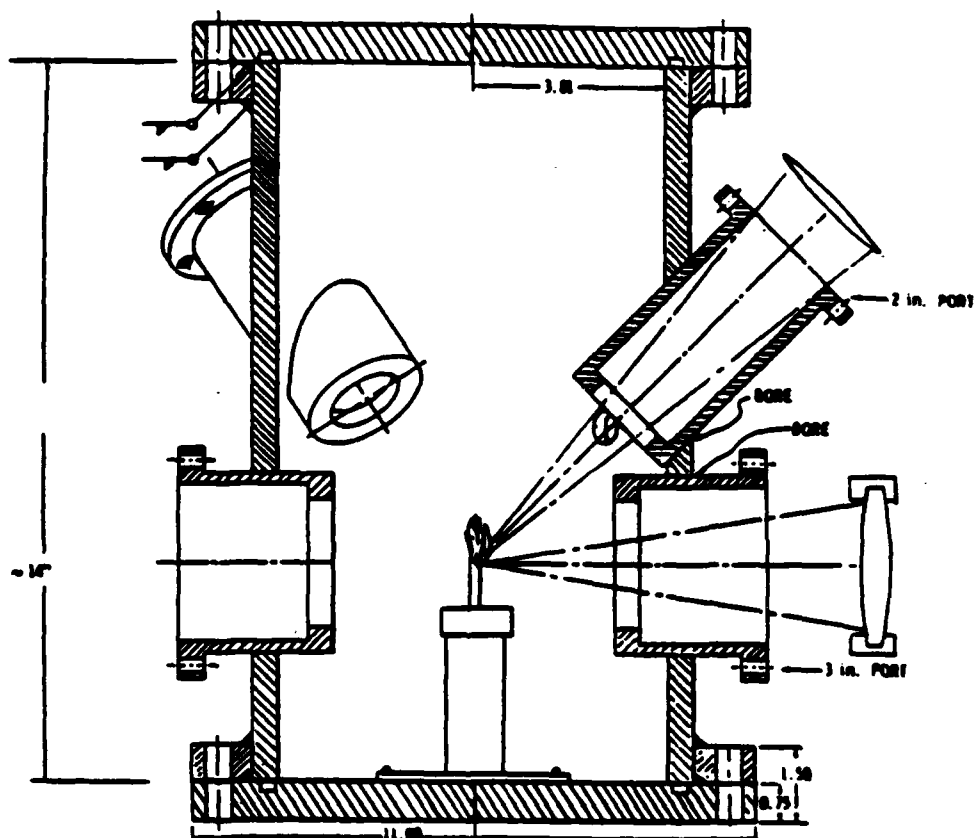


Figure 2. Cross Section of Window Bomb. The laser illumination is from the horizontal direction. The camera views the strands from a 45° angle, directly through the flame across the surface.

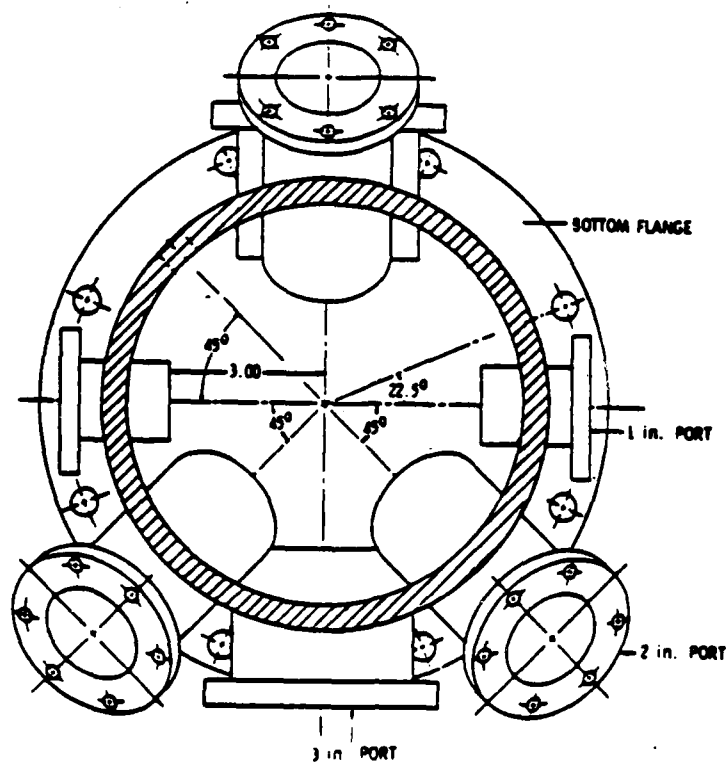


Figure 3. Top View of Window Bomb. Reentrant ports allow plentiful optical access while minimizing the size of the bomb.

extensive optical access, with ruggedness against window fouling, which is a special challenge for front-lit movies, since the camera must look down on the surface. The design chosen features several large reentrant viewing ports (Figure 4), allowing for optics as fast as f-1.3 to f-2. The chamber was made large (8 in. diameter by 14 in. height) to facilitate maintenance and minimize light attenuation from smoke. Problems with smoke were further reduced by the use of a high throughput purge that was primarily directed over the windows. The three ports on the back side of the bomb were provided for stereo photography. This window bomb has all the optical access needed for the experiment.

The pressure chamber was welded and stress-relieved. Welding distorted the ports by as much as 45 thousandths, more than had been anticipated. The seals on the windows only allow for variations in dimension of ± 0.005 inches. This necessitated remachining the ports and their sleeves. Chipping of the 2-in.-diameter BK-7 windows used in initial experiments was noticed. This chipping was probably due to radial stresses, and was in

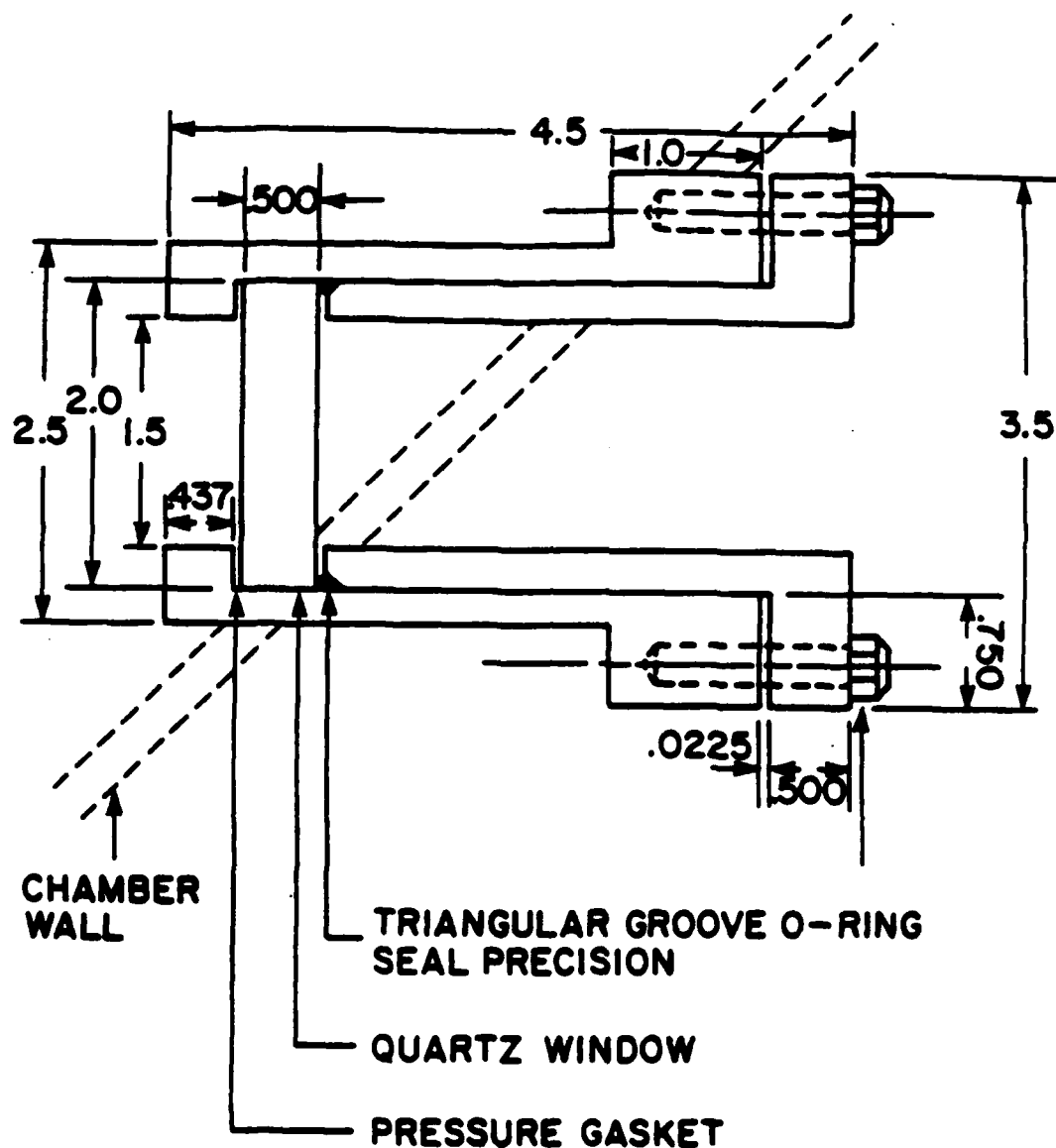


Figure 4. Reentrant Window Port. This design maximized optical access.

part related to the tight fit between the windows and the port sleeves. The chipped windows were replaced with quartz windows which were precision ground to match the port dimensions.

The interior of the chamber was painted with an epoxy coating to retard corrosion from the hydrochloric acid produced by strand combustion. An enclosure, built around the window

bomb, consisted of 2-in.-thick wood laminations; it was designed to yield, rather than rupture, should the pressure chamber fail. A secondary safety barricade was erected between the pressure chamber and the control area. The safety precautions included the purchase of ear and face protectors, miscellaneous safety modifications of the electronics and power supplies, and safety baffles to enclose the laser beam.

The window bomb design has allowed turnaround time between filmings as short as 30 minutes. In addition to reentrant windows with seals that allow for flexibility in viewing placement, other innovations in the chamber design include pressurization inlets at the chamber windows rather than at the strand, to minimize window fouling, and a mechanical strand mount to minimize turnaround time. A strand guide that minimizes frictional drag on the propellant was also developed; this allows the servosystem to make rapid corrections of the strand positions.

Due to the narrow (200-600- μm) depth-of-field restriction imposed by diffraction limitations and the high-resolution requirements, a rigid frame was built to hold the high-speed camera, window bomb, and servocircuit at fixed distances from each other despite their separation by one-meter distances. A thick metal table top and Unistrut frame supported the propellant combustion chamber on four adjustable legs. The thick metal plate served to focus and unitize the function of the other elements which completed the experimental setup. Two of the three legs of the camera tripod, the propellant-feed mechanism, and the servo-optics were also attached to this plate. The front pair of legs supporting the camera maintained a fixed film-to-target distance.

The third leg of the camera tripod, the propellant-feed mechanism drive motor, and several other items were also attached to the Unistrut frame using smaller metal plates. Thick rubber pads used in the construction of the camera tripod feet greatly reduced transmission of vibrations between the camera and propellant chamber/propellant-feed mechanism and other system elements. The camera/microscope assembly was rigidly attached to the tripod once proper alignment of the camera had been ensured. To minimize vibrations, the height of the unistrut frame was kept as low as possible. This was achieved by mounting the motorized translation stage in a horizontal position. Vertical motion of the strands was obtained by means of a triangular cam. This feature allowed lowering the overall height of the frame about 15 inches, improving stability. It also increased the stability of the mounting for the translation stage. In addition, a lower overall height facilitated operation of the system and added to safety.

The propellant was ignited using a wire filament and a high current pulse. A portion of the pressurizing gas that flowed

along the sides of the strand tended to break the ignition wires, so wires were made that were doubly wound except in their centers. The ignition wires were fastened to heavy copper leads that clipped in place and could easily be removed from the chamber.

The sides of the propellant were coated with an inhibitor to prevent flashing. The performance of traditional inhibitors, such as silicone grease, was not satisfactory for this work, due to smoke formation and incomplete inhibition. Testing of alternate inhibitors has shown that a partially reacted phenolformaldehyde polymer works very well as an inhibitor on propellant strands, provided that it is properly prepared with an appropriate solvent. (Ref. 22)

OPTICAL SYSTEM

Due to the high resolution sought and the physical limitations of the experiment, the work performed pushed physical limits. These limits and the optical design chosen are discussed in the following paragraphs.

Physical Limits

In the geometry used, the camera looked down on the strand surface through the flame and the laser illumination was directed from the horizontal direction. The strands were cut at a 45° angle to match the 45° viewing angle of the camera (Figure 2).

The standard method of dealing with film motion blur in conventionally illuminated high-speed photography is to use magnifying camera optics. (Ref 20) The blur as a percentage of the frame size remains the same, but the corresponding absolute size of the blur is reduced. For example, a magnification of four in a 16-mm film with a 1/100th shutter should give less than 20- μm of film blur. Additional advantages accrue from this approach, since the lenses in standard cameras, projectors, and enlargers do not work well at dimensions below about 25-40 μm , and the demands on film grain size and sensitivity are not severe using magnification. However, for a fixed frame size, magnification severely limits the field-of-view (to less than 2 mm in a 16 mm film using a magnification of four), a result contrary to our prime objective. Furthermore, the depth-of-field (the distance through which the object remains in focus to the camera) falls off inversely as the square of the magnification. High-resolution imaging requires fast optics. The f-number, f#, of a lens is given by the ratio of its focal length, f, to its diameter D:

$$f\# = f/D \quad (1)$$

The diffraction limited resolution, ζ , of an imaging system, is given by (Ref. 23)

$$\zeta = 1.2 f\# \lambda \quad , \quad (2)$$

where λ is the wavelength of the light used. At visible wavelengths with an effective $f\#$ of 8 the diffraction-limited resolution is about $8 \mu\text{m}$. The depth-of-field, z , is related to the resolution of the camera optics, b , by (Ref. 24)

$$z \sim f\# b \quad . \quad (3)$$

If b is at the diffraction limit, ζ , this gives

$$z \sim 1.2 f\#^2 \lambda \quad . \quad (4)$$

For a resolution of $20 \mu\text{m}$ and an $f\#$ of 8, z is on the order of $160 \mu\text{m}$. This can be significantly less than the dimensions of the larger particles, let alone the large-scale variations in surface topography due to the vagaries of heterogeneous combustion. The depth-of-field limitation becomes even more stringent with magnification. For a given magnification, M , Equation (4) is modified to

$$z \sim 1.2 (f\#/M)^2 \lambda \quad . \quad (5)$$

Since the depth-of-field problem is aggravated by flame turbulence at pressure, due to changes in the optical path length, magnification virtually precludes movies of extended length on fully combusting surfaces of appreciable area. Of course, for a fixed film frame size, the field-of-view also decreases as $1/M^2$. (Ref. 23) For the above reasons it is often preferable to demagnify rather than magnify the film images. This approach places heavy demands on the quality of the camera lens and the resolution of the film used, as well as on any lenses used in the reproduction or projection of films. Although it has been possible to obtain useful quantitative data using demagnification, the resulting films lack visual clarity. The production of movies with easily discernible features requires high-contrast images, which are especially difficult to obtain from a low-contrast subject. The problem of preserving image contrast leads to the concept of the Modulation Transfer Function.

All lenses, as well as photographic film, act as low-pass spatial filters; i. e., the signal from small features is severely attenuated relative to the signal from large-scale objects. The surfaces of the propellant strands on which our experiments are made have little contrast. As such, the movies of their deflagration are especially affected by the falloff in contrast of any optical system with the inverse of the spatial dimension of interest. The inverse of the spatial dimension is referred to as the spatial frequency, k . The reduction in image

contrast due to the low-pass behavior of the lens and film is described by the Modulation Transfer Function (MTF). (Ref.24) Since any object, such as a standard bar chart, can be represented by a superposition of cosine fringes, we consider a cosine fringe pattern of frequency k represented by $I(x) = 1 + m \cos(2\pi kx)$.

The modulation is defined by

$$MTF(k) = \frac{I_{max} - I_{min}}{I_{max} + I_{min}} = \frac{(1 + m) - (1 - m)}{(1 + m) + (1 - m)} = m \quad (6)$$

The modulation m is equivalent to the fringe contrast. When the fringes are imaged or recorded, their modulation is attenuated by an amount which depends on the fringe frequency. This attenuation factor is the MTF of the lens or film under consideration (Figure 5). The absolute upper frequency limit on the MTF for a lens is set by the lens aperture-film combination.

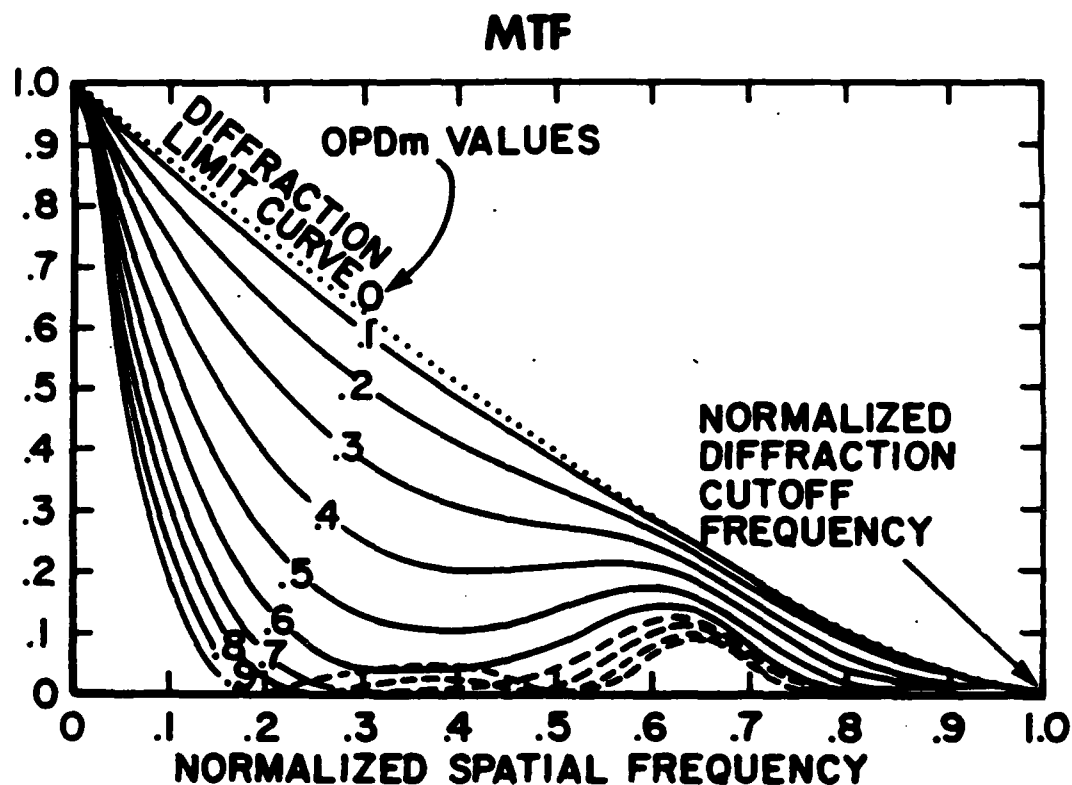


Figure 5. Modulation Transfer Function of Typical Single-Element Lens. Note that the monochromatic curve is vastly superior to the polychromatic curve. Reprinted with permission of Melles Griot Corporation, Ref. 2.

The cutoff frequency of the camera system, k_c , is given by

$$k_c = \frac{1}{2\lambda f\#} \quad (7)$$

A lens will have an MTF that decreases to this limit. Obviously, if the contrast of the subject is less than one initially, a small value of the MTF will drive the resultant contrast of the image below the detection limit, well before the frequency cutoff of the MTF is reached. Typically a much lower spatial frequency, k_1 , will apply, since the quality of the image will degrade steadily as k_1 increases, especially with low contrast object fields. Often k_1 is taken to be about $k_c/4$. The required relation for ζ at a given magnification M is: (Ref. 25)

$$\zeta = 1/Mk_1 \quad (8)$$

Therefore, it is desirable to maximize k_1 . Unfortunately, z obeys the relation (Ref. 25)

$$z = \frac{1}{(Mk_1)^2} \frac{1}{\lambda} \quad (9)$$

for light of wavelength λ . Therefore, high-resolution movies with a practical depth-of-field must be made at low magnification. Note that z and ζ are coupled, with

$$z = \zeta^2/\lambda \quad (10)$$

This places severe limits on the system as ζ approaches λ . To complicate matters, the overall MTF of a system is the product of the component MTFs, as very high quality components must be used at every step. This includes the MTF of the film (Figure 6). Please note that MTFs are much worse for white light than for monochromatic light (Figure 7).

As a rule of thumb, the highest usable frequency passed by an optical system is about one fourth of the usable MTF cutoff. The detection limit of the system is the inverse of the usable MTF cutoff. To be resolved, an object should be twice as large as the detection limit, and to be well resolved it should be four times as large as the detection limit. For example, to image a 20-micron object, at least a 10-micron resolution is desired, which corresponds to 100 line pairs/mm. Ideally, the MTF of the imaging lens should even extend out to 400 line pairs/mm. At $\lambda = 0.51$ microns (the copper-vapor wavelength) the lens should ideally operate at an $f\# = 2.5$. A trade-off must often be made between detail in a film and visual quality. Low-contrast features are most severely affected by the fall-off of a lens/film system MTF with decreasing feature size, so that small-scale, low-contrast details tend to blur out. Large-grain film and a high-contrast developer result in a film with good visual clarity, while a fine-grain film and a soft developer give a more faithful representation of the object field. Similar

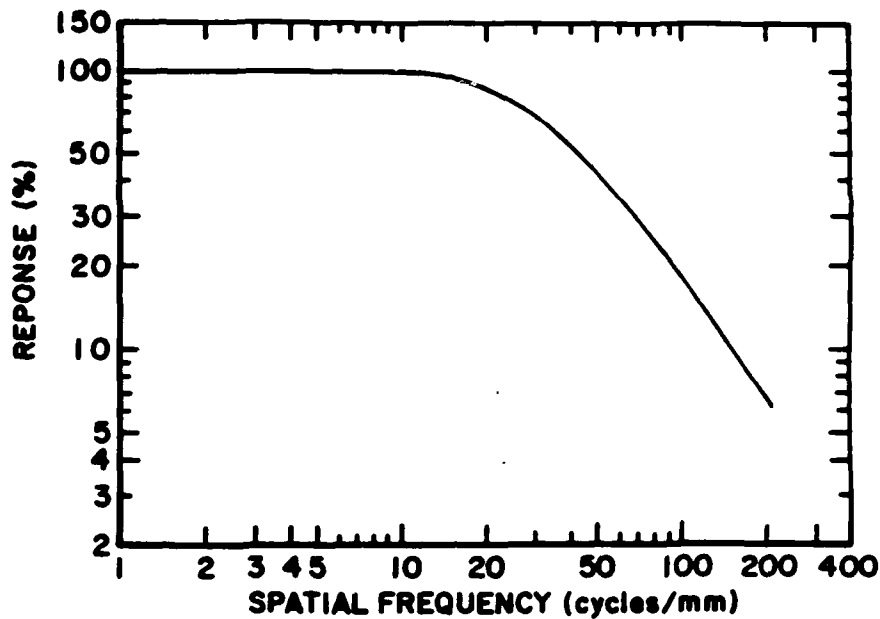


Figure 6. Modulation Transfer Function (MTF) of Film. This low-pass curve is multiplied by the MTF of the camera lens, impairing the contrast of the features. Adapted from Eastman Kodak.

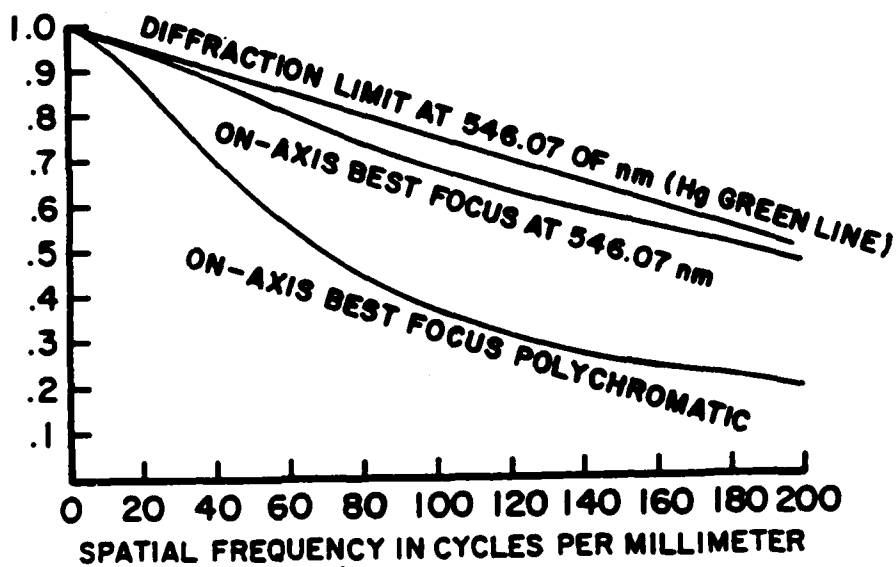


Figure 7. Modulation Transfer Function of White Light vs. Monochromatic Light. Due to chromatic aberrations, superior contrast can be preserved with monochromatic light. Adapted from Melles Griot Corporation, Ref. 2.

considerations apply to reproductions, whether by motion picture projectors or enlargements of individual frames. The fine detail obtained in a soft picture leads to a blurred result in reproductions using standard commercial equipment.

The best MTFs can be obtained for an optical system which is very close to the subject, as in a microscope. Unfortunately, very small object distances are not practical in combustion photography. The need to protect the camera lens, the need to obtain a reasonable depth-of-field, and constraints imposed by the design of a camera at unity magnification require a minimum object distance on the order of 100 mm. Provisions for such a minimum distance were made in the design of the window bomb. Using standard high-quality optical glass, this constraint and the need for a manageable depth-of-field lead to a maximum lens f-number of about 6-7. At unity magnification this would give a cutoff spatial frequency of about 150 line pairs/mm. Smaller lens f-numbers cannot be used since they would seriously impair the depth-of-field.

The MTF falls off rapidly as the field-of-view is increased (see Figure 8). For a 1/8-inch radius and a 5-inch object

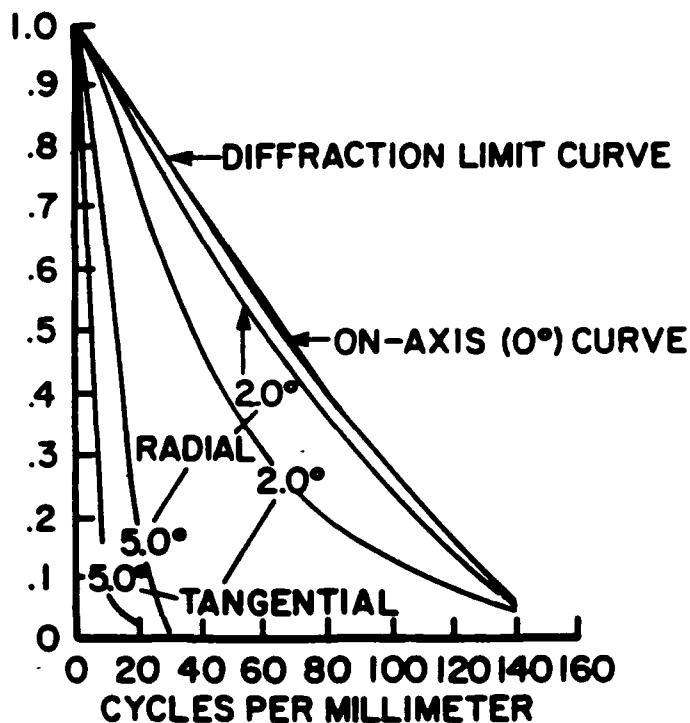


Figure 8. Modulation Transfer Function vs. Field of View.
Performance falls for non-paraxial rays.
 Reprinted with permission of Melles Griot Corporation, Ref. 2.

distance the paraxial angle will be as much as 1.5°. This poses no severe difficulties for monochromatic light. However, it seems that an enlarger lens and a projector lens should be designed for large image distances. A curved screen may be helpful for movies.

Degradation Due to Flame Turbulence

The degradation of the image of an object field due to random density changes in the intervening gas is a topic which has been extensively studied in statistical optics. As in the case of the analysis of the requirements on the camera optics, it is best described in terms of a transfer function and spatial frequencies. Suppose we wish to discern a feature on the surface of the propellant of size Δx . The associated spatial frequency, k , is given by

$$k = 1/\Delta x \quad . \quad (11)$$

If the variance in the deviations of the optical wave front emerging from the propellant surface due to flame turbulence is s^2 , then the transfer function which describes the fall-off in contrast with increasing k is given by

$$T(k) = \exp[-k^2 s^2] \quad . \quad (12)$$

This means that the contrast of a picture falls off extremely rapidly as the wavefront distortions due to flame turbulence increase and/or the size of the feature of interest decreases. The fall-off is so strong that the retrieval of fine detail rapidly becomes impossible with increased operating pressure.

Note that a given value of the transfer function depends only on the product ks . Therefore, whatever level of visibility is chosen as acceptable, the size of the minimum feature that can be discerned should scale inversely with s . Assuming that the mean scale of the wavefront distortions due to flame turbulence scale as the pressure, the minimum size of features which can be resolved in experiments on 1/4-inch strands is estimated as follows:

p (psi)	200	300	400	500	600	800
x (microns)	15	20	30	40	50	60

These values hold only for ignition movies. As the propellant surface heats up following ignition, flame turbulence becomes worse, and the above values for minimum feature size should be increased by a factor of three. Some improvement can probably be achieved by choosing camera optics that maximize depth of field rather than resolution. There is little point in using fast optics if flame turbulence wipes out fine features. Increasing the depth of field would at least bring a greater portion of the strand surface into focus.

Optics

All of the movies in the experiment were made at a magnification (M) of 1 or 0.5. The depth-of-field was estimated as less than 200 μm at unity magnification and about 600 μm using a demagnification factor of two. A Nikon 50mm Nikkor f-4 micro lens was used in the initial experiments. This lens was rated at a resolution of 100 line pairs/mm and was tested at a resolution of 6 μm on high-contrast images. Unfortunately, most of the propellants studied have low-contrast surfaces in the absence of any contribution from flame emission. Consequently, the MTF of the lens-film combination limited the best resolution to about 20 μm . Typically, the smallest identifiable features in these films measured about 25 μm . The Nikkor lens was designed for operation in a demagnifying configuration with a demagnifying ratio of 2:1. Most of the movies using the Nikkor were filmed in this demagnifying configuration to extend the depth-of-field. Films of strand ignition on stationary propellants were made at unity magnification using an additional lens element. This resulted in a further degradation of the MTF of the camera lens.

The Nikkor lens was subsequently replaced with an f-6 lens made by Rodenstock. This lens is of extremely high quality and produced movies with a resolution of 15 microns until flame turbulence became a problem--generally at pressures above 200 psi. The Rodenstock lens was mounted directly inside the lower 3-in.-diameter port immediately outside of the port window. In the experiments using this lens the camera was mounted in front of the lower 3-in. window, and the laser beam entered from the upper 3-in. window. This configuration is similar to the one used at China Lake.

The sighting scope on the camera was inadequate for proper focusing on microscopic targets. A new sighting scope was designed for the camera, since the existing sight did not possess sufficient resolution to achieve satisfactory alignment. This scope used a microscope objective mounted behind the camera. The location of the focusing scope relative to the camera was maintained by mounting to a heavy (1/2-in. thick) aluminum plate.

Laser speckle is a common problem in high-resolution photography. Film tests showed that the copper-vapor laser had sufficient coherence to induce laser speckle. This problem was met by inserting an ellipsoidal coherence spoiler in the input optics (Figure 9). The 510 nm copper-vapor laser light was focused on a stainless-steel ball coated with magnesium oxide powder. The light scattered by the rough surface of this ball was collected by an ellipsoidal mirror and focused on a target. The spoiler has been tested using both a 632.8 nm He-Ne laser and the copper-vapor laser. The spoiler succeeded in eliminating almost all of the speckle from the He-Ne laser--a severe test. It was found that, due to the semitranslucency of the AP propellants, speckle was not in fact a difficulty, and the spoiler was removed in the experiments using the f-6 lens.

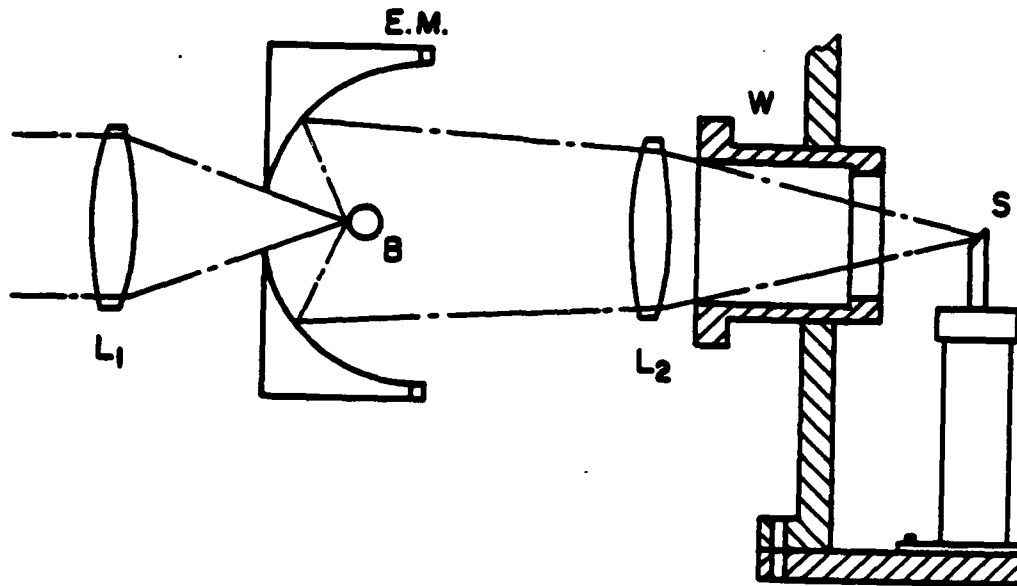


Figure 9. Coherence Spoiler. The large focusing angle given by the ellipsoidal mirror and the powdered surface of the ball at one of the mirror's foci successfully eliminate laser speckle.

SERVOPOSITIONING CIRCUIT

A servopositioner was developed to locate the position of the surface of a strand of rocket propellant as it burned in an irregular fashion. (Ref. 26) A concomitant of high resolution in a photograph is a very shallow depth-of-field. (Ref. 27) In this case, the depth-of-field was sometimes as small as 200 microns. Since the propellant burned at a rate of one to four centimeters per second, only about two-hundredths of a second were available during the course of a normal burn in which the propellant would be within the proper depth-of-field. However, because it was desired to take movies over a period of several tenths of a second, it was necessary to continue to push the strand forward to maintain the surface within the depth-of-field. This task was not simple, because propellants burn in a highly irregular fashion and there are local irregularities on the heterogeneous surface itself which can be as much as 400 microns in size. Hence, it was necessary to design a circuit which could compensate for the motion of the burning strand and the idiosyncracies of the mechanical drive, and continue to locate and hold smoothly the position of the surface to very tight tolerances.

The problem is made more difficult because intense smoke is generated by the burning of the strand. This smoke interferes with the intensity of a laser light beam used to sense the position of the burning strand, and furthermore the smoke will foul windows used in the pressurized chamber. These problems make use of a single-detection element unsuitable, as that detection element would then become sensitive to the amount of smoke and the amount of fouling of the windows, rather than to the true position of the strand. For this reason, as a sensing element an array of photo-diodes was chosen, each of which had a given threshold level, above which the diode would fire and produce a unit signal. The total signal determining the position of the strand then was given not by the total light level falling on the array, but by the number of diodes in the array which were either on or off.

Previous opto-mechanical servocontrol units used only one or two photo-diodes as detection elements. (Ref. 28) As such, they were not highly rugged to smoke or window fouling, and had fundamental limitations on the tightness with which they could control the location of the target. They had no special optics for controlling the range of the target or eliminating flame luminescence. They were limited in their ability to follow an irregular moving object. By contrast, the circuit used here was insensitive to flame illumination, smoke, and turbulence, was highly agile, and afforded excellent position control.

Opto-Mechanical Subsystems

Our system had three parts: an optical part (Figure 10), a

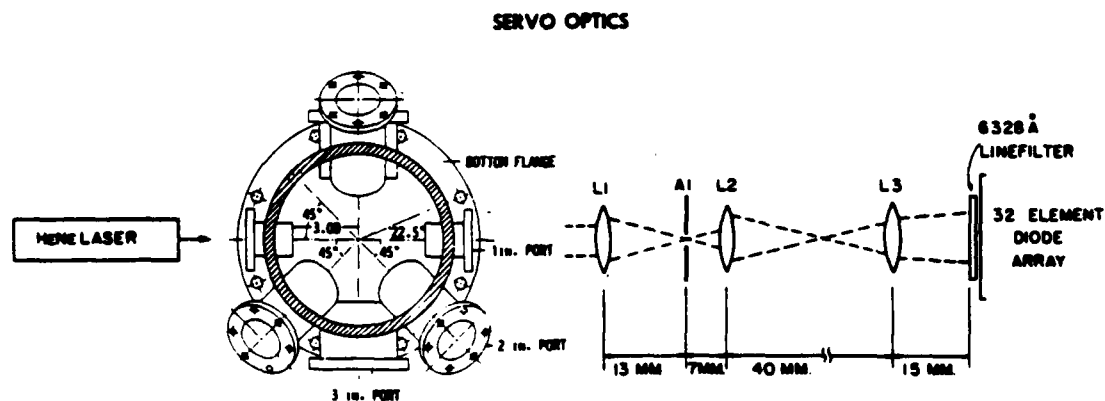


Figure 10. Servooptics.

mechanical drive (Figure 11), and an electronic circuit. The fuel-feed mechanism consisted of a nonrotating, ball-bearing-guided push-rod attached to the underside of the chamber mounting plate and a motor-driven triangular cam attached to a Unistrut

MECHANICAL DRIVE MECHANISM

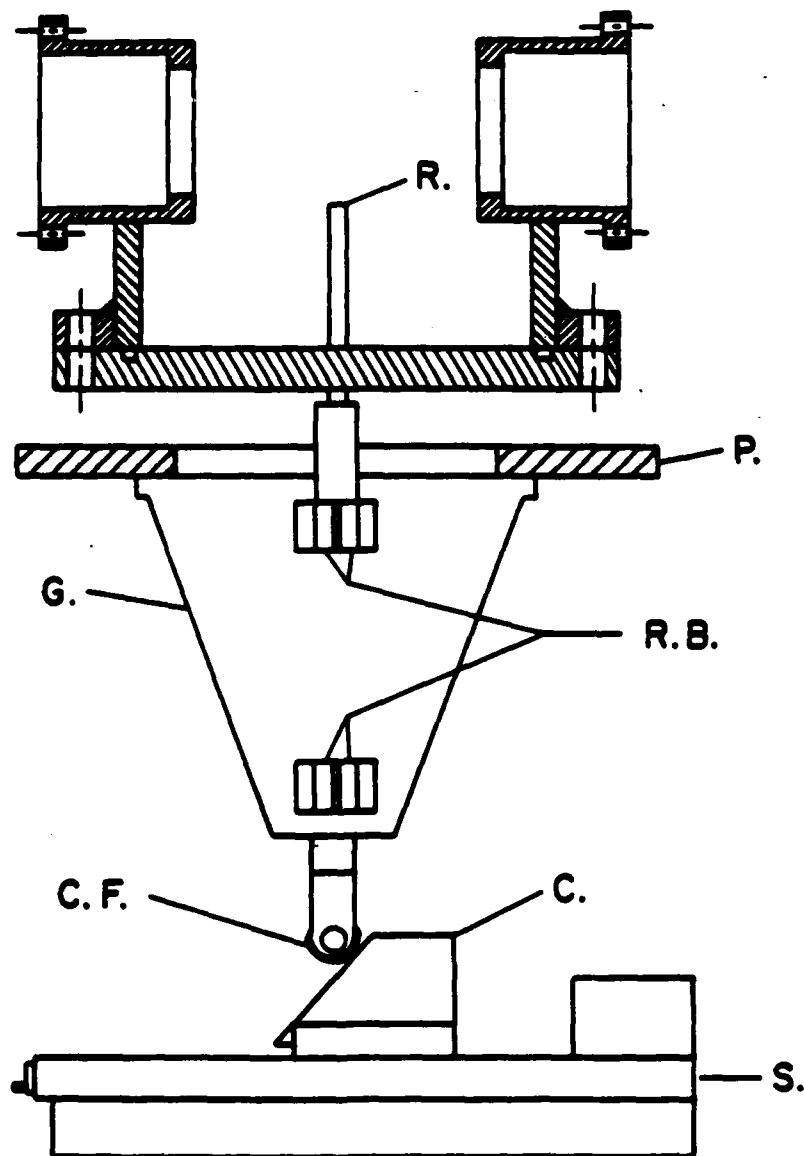


Figure 11. Mechanical Drive for Positional Controller

frame. A maximum push-rod stroke of two inches was possible. The push-rod rate of advance, as a function of motor speed, could be varied by changing the wedge-shaped cam shown below the roller bearing at the end of the push-rod. The ball-bearing guide ensured that the push-rod will move smoothly without flexing under the horizontal load of the translation stage. The stage mounting block was adjusted and a mount for the entire motorized assembly was built to ensure a smooth drive of the strand shaft. The limiters were removed from the control box, which increased the rate at which the servomotor could respond.

The diode array detector for the proportional drive servocontrol was a circuit (Figure 12) which provided information on the position and velocity of the irregularly moving surface. Ablating propellant surfaces have erratic trajectories and need to have their position compensated if a smooth trajectory is desired. In many cases, this is relatively simple to achieve, but this circuit dealt with a case in which there was a great deal of noise on the information channel providing the instantaneous location of the surface and the trajectory was in fact highly erratic. In these cases, if tight control is desired, it is necessary, due to an inherent lag in any mechanical control of the surface, to anticipate the motion or future position of the surface to be controlled. This required the ability to derive the surface velocity. There were not enough elements in the array to make an accurate determination of the acceleration. This circuit totaled the signal from an array of sensing elements, each of which was either in an "on" or "off" mode, depending on a threshold level set for each level of the signal input to each sensing element. Use of an array of on or off sensing elements is especially helpful in cases where the signal channel is subjected to noise. Since an optical signal was employed and the optical path was subject to interference from smoke or dirt on windows, this system was especially rugged. The circuit was especially useful in conjunction with a proportional control on the mechanical part of the servosystem. This helped to avoid overshoots and erratic motion. In brief, this circuit involved a multielement, nonlinear servocontrol which incorporated all the peculiarities of the entire servosystem in its calculations.

Each element or pixel in the array corresponded to a surface displacement of 50 μm ; consequently the capture range for the system was about 1.6 mm. The circuit made use of two input signals: the location of the surface, and the time integral of the difference between this location and a reference position (error signal). The servocircuit sensed the position of the strand surface and provided a reference voltage to the controller on the slide motor. It had a proportional drive based on individual on/off signals from 31 elements in a photodiode array. These features provided a smooth control and resistance to fouling of the windows.

Control Circuitry

The servoposition controller was made up of three printed circuit boards (Figures 13-15). The first was the detector and analog conditioning board (Figure 13). The second board was the

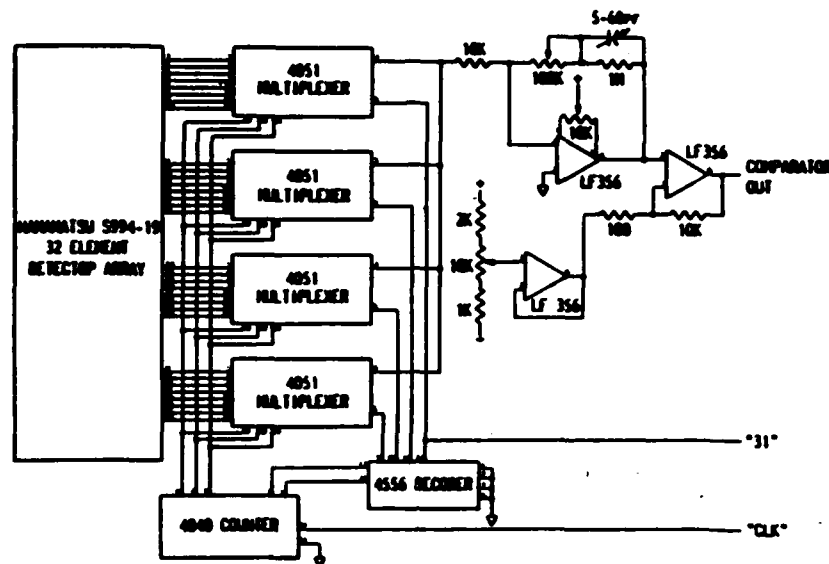


Figure 13. Detector and Analog Conditioning Circuit. Each detector element is sequentially switched to an amplifier and level comparator.

digital processing board (Figure 14), and the final board (Figure 15) was the analog controller. The output from the analog controller board drove the slide controller. The slide controller moved the propellant strand up as the propellant burned down to maintain the burning surface at the same position relative to the camera lens. The detector was a Hamamatsu S994-19 32-element array. Since 0 V is a valid signal, the number of possible data outputs is equal to $N + 1$, where N is the number of photodiode elements used. Since the computer could only accept 32 possible input voltages, only 31 of the 32 elements in the photodiode array were actually used. Each detector element generated a positive voltage when exposed to light. The analog processor board sequentially switched each detector element to an amplifier and level comparator. If the light level on a detector element was above a preset threshold, the output was high; otherwise it was low.

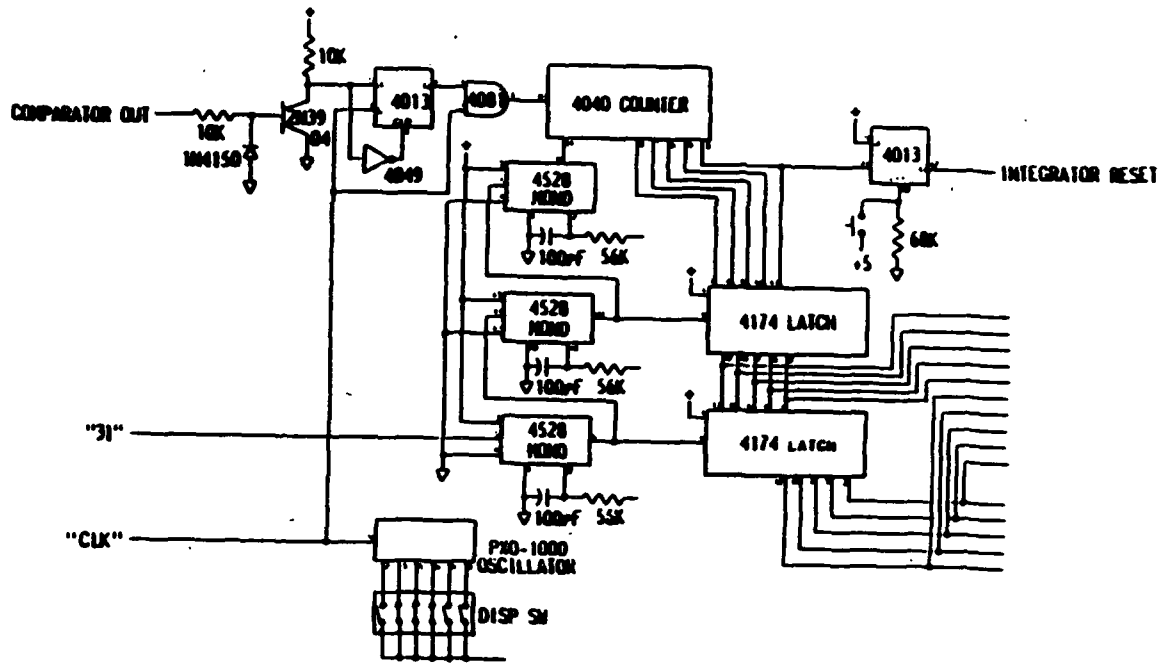


Figure 14. Digital Processing Circuit. The number of elements above threshold is counted and stored.

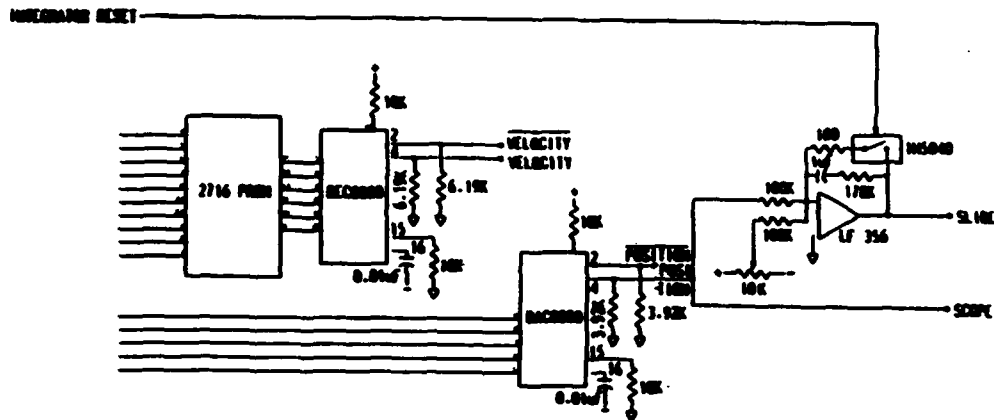


Figure 15. Analog Control Circuit. Each detector element is sequentially switched to an amplifier and level comparator. A PROM takes the difference between two latch outputs to form a signal voltage.

The second board took this signal and counted the number of elements above the threshold. When 31 elements had been compared with the threshold, the value of the counter was stored in the first latch, after the previous value of the first latch was saved in the second latch.

The third board took the outputs from the latches and used a programmable read-only memory (PROM) to take the difference between them. The difference was proportional to the velocity error between the slide and the burning propellant. The output of the first latch was proportional to the positional error of the propellant.

In this circuit implementation, only the position error was used as an input to the analog controller. The controller consisted of an integrator, with a resistor in series with the feedback capacitor to provide damping. The setpoint and signal were connected to the inputs. The difference between the input and setpoint was integrated and the resultant integrated difference signal was used as the proportional input to drive the slide controller. A flip-flop was held in the reset mode when the manual reset switch was depressed. This flip-flop controlled an analog switch which held the integrator in a reset mode. When the detector changed from more than half dark to less than half dark, the flip-flop toggled, and the circuit started in the controlling mode.

The main nonlinearity in the system was due to the difference in velocity between the forward and reverse directions, because of the unidirectional drive on the slide. The servocontroller regulated the slide velocity in only one direction (the difference between the burn velocity and the slide velocity), whereas the velocity in the reverse direction was determined solely by the burn velocity of the fuel. These differences placed constraints on the servocontroller design. Another source of nonlinearity was the detector. The spacing of the detector elements might have been nonuniform, resulting in a nonlinear positional response. The sensitivity of the individual photodetectors was also subject to variations, as was the energy profile of the laser, resulting in a shift of the detector threshold that could produce a positional nonlinearity.

To start a test, the propellant strand was positioned so that more than half of the detector elements were dark, the reset switch was depressed, and the slide controller was turned on. When the propellant burned down, exposing more than half of the elements, the flip-flop was toggled and the integrator was allowed to operate.

An early version of this circuit used only 8 elements in the photodiode array (Figure 16). The 8-element diode array performed unsatisfactorily because the capture range of the array was too small and the attempted precision was too great.

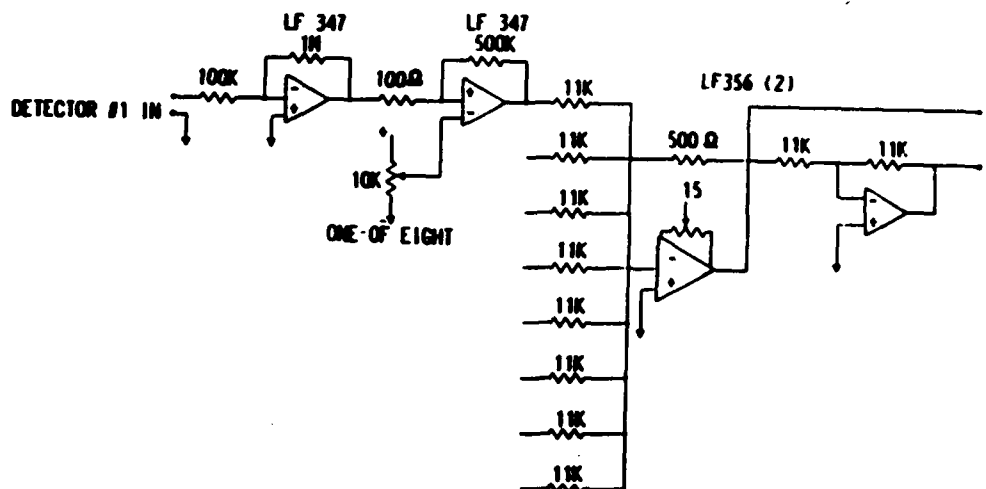


Figure 16. Eight-Element Circuit Prototype. The limited number of elements reduced the capture range and precision of the system.

Increasing the number of elements used in the detector circuit from 8 to 31, and increasing the distance surveyed by each element from 25 μm (0.001 in.) to 50 μm (0.002 in.) increased our capture range from 100 μm (0.008 in.) to 1.6 mm (0.064 in.). Tests showed control to within two pixels, or 100 μm . Attenuation of the 632.8 nm He-Ne laser beam due to smoke corresponded to a signal drop of less than 50 mV. The voltage to each diode in the array was about 80 mV, so beam attenuation due to smoke corresponded to a position error of less than 50 μm . Initial immunity to fogged windows was not as great as we had hoped, possibly due to marginal (2 mW) laser power. Fouling of the windows was subsequently minimized by directing part of the pressurizing gas directly over the window (the bomb uses a continuous flow of pressurizing gas). (Ref. 22)

Servoperformance

Since the photodiode array was only one-dimensional rather than two-dimensional, errors in the mean position of the strand profile occurred if the profile changed. This problem was alleviated by igniting the surface at the short side of the profile (strands were cut at 45° angle) and by using a special non-smoking, nonflaking inhibitor that matched the propellant burning rate. (Ref. 22)

Due to a time lag produced by the slide and its motor, the system went into oscillation if the performance specifications were made too tight. The error signal was used as the main drive

signal and the instantaneous position was used to estimate an appropriate damping factor for the drive signal. The thresholds for the diodes were adjustable, as were various other circuit parameters. The system was optimized for burning rates between 0.3 and 1.5 cm/s.

The velocity of the surface could not be used as a third input signal, because the limited number of diodes in the array led to a heavily digitized velocity reference signal. The servocircuit was subject to radio frequency (rf) pickup from the pulsed copper-vapor laser used in the photography experiment. The ground on the servologic circuit was improved and rf pickup was reduced to 50 mV. Difficulties arose with the range of control of the servopositioner as the chamber pressure was increased. Subsequent to extensive testing, it was determined that although the servosystem could benefit from improved optics and more elements in the diode array, the most serious problem was with the motor controller and the slide--particularly the slide, which had too much friction. Additional improvement in performance resulted from reducing the weight of the slide bar.

Focusing film was put into the camera and the image of the strand surface was observed during test burns. Repeatedly the surface receded from view even though a scope trace indicated that the servocircuit was holding the strand surface in position. It is believed that the strand flame forms a thermal lens which deflects the servolight beam upwards slightly. This effect would vary from burn to burn, but it apparently increases as the surface moves further from the laser beam. The effect is small and is only troublesome when very tight tolerances are required. Three corrective measures can be applied to the problem. The first is spatial filtering in the collection optics, since the dc component of the servosignal should be the least sensitive to a schlieren effect. The second is the use of an incoherent servobeam, with a large convergence angle. An attempt was made to apply spatial filtering and incoherent optics to the servosystem, but it was found that due to the limitations of the one-inch servoports, sufficient signal strength was impossible. Using 2-in. servoports, it should be possible to make use of optics to spoil the coherence of the servolaser beam without significantly reducing the beam power. The third measure is injection of the pressurizing gas through a tube surrounding the lower end of the strand, to control the flame profile.

Local Burning Rate

The mean, time-averaged burning rate is usually not a fully satisfactory parameter with which to specify a propellant in a motor design. Practical propellants have a dynamic response to the chamber flow. (Ref. 8, 29-31) An important example is the response of the burning rate to small-amplitude pressure oscillations. This acoustic response can have a critical bearing on the stability of a rocket motor. The acoustic response

includes information in the chamber pressure; that is, it contains phase as well as amplitude information, and is a complex quantity. Ideally, both the real and the imaginary parts of this response function are desired.

Although the mean burning rates of propellants are reasonably well known, no quantitative means is used to measure the local instantaneous burning rate. This is unfortunate, as the latter parameter is the one of greatest importance in dynamic phenomena. Traditionally, acoustic response functions have been measured using specially configured burners known as T burners and L burners which are expensive to operate and difficult to calibrate. (Ref. 32-35) The information obtained from them is indirect, has poor resolution, and suffers from a high degree of uncertainty. These burners provide little input on the imaginary part of the response function. Moreover, traditional measures of the acoustic response function have been global measurements. A technique which measures the response on a granular level should be of superior use in understanding the factors responsible for a propellant's oscillatory response. This would entail a study of the local regression of a propellant and its time dependence in the presence of a strong pressure oscillation of known frequency. Both the phases and modulus of the oscillatory regression rate in relation to the acoustic pressure oscillations would be desired.

We have developed and demonstrated a quantitative system for measuring the burning rate along a given line on the surface. This capability is a spin-off from our servopositioning development work. The diode-array output of the servocircuit gives a record of the position of the strand surface where it intersects the servolaser beam. We have shown that this record can be used to track the motion of the surface (see Figure 17). Essentially, this experiment is a back-lit system with a photoelectric detector in place of film. The data may be used without attempting to control the strand position, greatly simplifying the required circuitry. The 31-element linear array used in our system could be extended. More elements in a linear array would provide more detailed information over a long time period. A two-dimensional array would give information on the correlation of local burning rates at different positions.

The data obtained in this manner do not reach the ideal objective of a fully localized burning rate, i.e., approximately "point" information. Rather, they yield an integral of the burning rate along the line formed by the path of the laser beam. However, this rate is certainly a more localized than a rate obtained by integrating the burning rate over the entire surface area. Even more localization can be obtained by burning strands that are peaked at their centers. Above all, this method yields an instantaneous burning rate, which is of greater interest since it is at least partially localized.

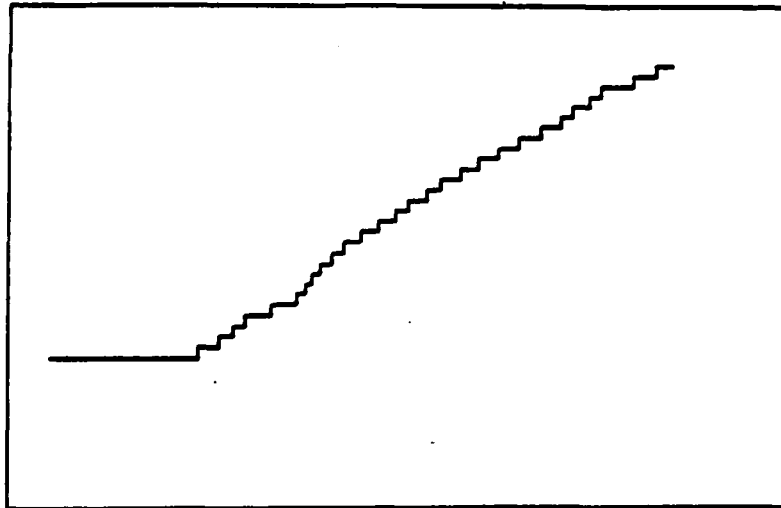


Figure 17. Photodiode Array Trace Showing Surface Location vs. Time.

LASER DEVELOPMENT AND SYNCHRONIZATION ELECTRONICS

The experiment would not have been possible without the development of a novel circuit for synchronizing the pulses of the laser to the framing rate of the camera. This circuit and various improvements made on the laser itself are described in the following paragraphs.

Pulse Synchronization Circuit

An electric circuit was built to provide a trigger pulse in synchronization with the motion of the high-speed camera whose velocity was not constant, i.e., the camera was accelerating (Figure 18). (Ref. 36) It also provided an automatic transfer from a mode in which the trigger pulses occurred at a constant rate to one in which they were synchronized with the motion of the non-uniformly moving camera. The copper-vapor laser was heated (and heat was essential to its function) by the electrical discharges in the pulsed operation of the laser itself. The laser was designed to run at an average repetition rate of 5000 pulses per second. Unfortunately, the high-speed camera used in the photography did not have a consistent velocity. Therefore, if the pulsing of the laser were not synchronized with the framing rate of the camera, the pictures taken would not have been matched to the center of the frame on the camera. Consequently, they would be impossible to interpret when a movie was played back. Therefore, it was necessary to synchronize the pulsing of the laser with the framing rate of the camera. It is to this end that the pulse synchronization circuit was developed.

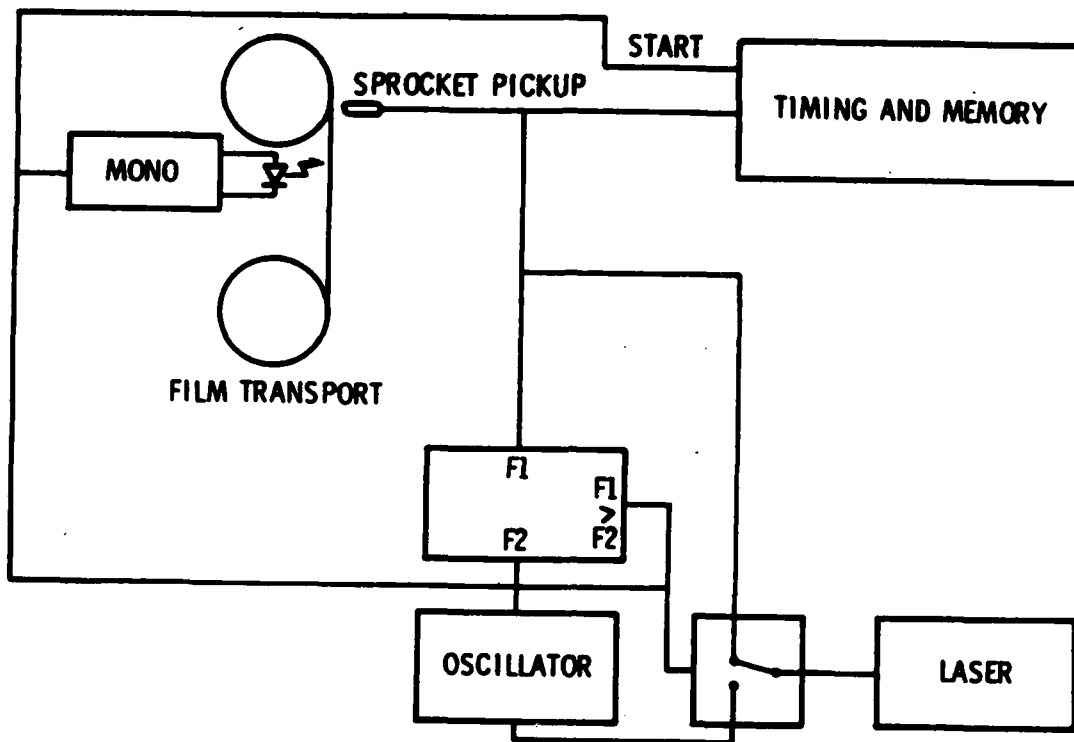


Figure 18. Pulse Synchronization Block Diagram. This circuit automatically switches the laser pulse rate from a free-running value to one which matches the camera framing rate.

The synchronization of a light source and a camera has been done routinely with a high-speed xenon flash lamp. This can be done for a single flash or for repetitive flashes. Due to significant differences in their mode of operation, synchronization of the high-speed camera with the copper-vapor laser presented a serious problem. The copper-vapor laser was self-heated by the electric discharge. The laser was started and warmed up on a free-running oscillator. The high-speed camera frames at an accelerating rate. When the high-speed camera's framing rate was up to this speed, the laser was driven from the camera. At the end of the film, the camera was shut down and the laser was switched back to the free-running oscillator.

The frequency at which the laser was switched over to the camera was determined by the free-running oscillator frequency. When the camera framing rate was equal to the oscillator frequency, the circuit skipped one camera pulse and switched to the camera. This was necessary to prevent the thyatron-triggering circuit in the laser from being double pulsed, causing

it to latch up and stop lasing. While the laser was being triggered from the camera, the oscillator frequency was shifted down by about 200 Hz. This hysteresis prevented the circuit from switching between the camera and oscillator due to small changes in the camera speed. When the camera ran out of film, the reverse operation occurred and the laser switched back to the oscillator.

The timing pulses to the synchronization circuit were obtained from a magnetic pickup transducer located in the camera that sensed the proximity of the sprockets that wound the film. Timing marker pulses were made on the film via an LED and fiber optics. The phase relation was adjusted between the location of the film sprocket holes during runs and the firing of the laser by adjusting a mount for the magnetic pickup transducer in a trial-and-error procedure. Due to its close proximity to the camera motors, inductive noise pickup from motor transients was severe. Consequently, a grounding rod was installed and noise from the laser and its power supply was substantially reduced. The installation contributed greatly to the improved performance of the synchronizing circuit, which subsequently worked satisfactorily.

Copper-Vapor Laser Development

Several copper-vapor lasers have been designed and built at UDRI. An early version of a commercial laser was used for high-speed combustion photography. Since this was really an experimental version of the product, it was necessary to make a number of improvements to the unit. The laser power supply and the head were modified to minimize the possibility of damage due to failure in the cooling system. The Tygon water lines have been replaced with nylon lines, allowing for a higher temperature and pressure margin, and a temperature-sensing interlock has been installed in the power supply. Improvements in various grounds and insulators have resulted in reduction in the frequency of occurrence of laser lockup and stray timing markers. The laser head has been subject to frequent high-voltage breakdowns. Part of this is an rf breakdown, due to the intense fields generated in the 100 MW breakdown discharges in the plasma tube. The fundamental frequency of this rf field is about 30 MHz. The laser head is too small, making it difficult to isolate electrically the various components crowded within it. A recommendation was made to the laser manufacturer that they increase the size of their chassis for the laser head. They agreed, and have since increased it to 10 inches in height and 16 inches in width in their newer units.

In the course of this work, we made the following recommendations, all of which have been adopted by the manufacturer:

- Replacement of the Buna-n "O" rings with Viton "O" rings;
- Antireflection coating of the windows;
- Strengthening of the insulating spaces in the laser head;
- Shock-mounting of the components in the power supply;
- Strengthening of the internal connections in the power supply;
- Changing the location of the gas and vacuum valves in the laser heads to reduce hazards during turn-on and shut-down.

As expected with new products, there have been several maintenance problems with the copper-vapor laser. A fault in the thyatron driving frequency circuit caused fuses and components to blow. In succession, a transformer, a resistor/diode chain, and a driver tube blew in the driver circuit. A large capacitor in the laser head leaked oil and exploded when the oil reached ground, spraying glass and oil around the laser head. A lead to the bleeder resistor in the head was never properly secured during installation. The lead broke free, producing a short, which set afire some oil remaining from the leakage of the main capacitors. The mylar insulation being used then caught fire and burned out the wiring around the thyatron. It was necessary to remachine the mounts for the capacitors, install capacitors which were resistant to leaking oil, rewire and replumb the laser head, and replace the mylar insulation with pyrex and fiberglass insulation. Unfortunately, the repair was very time consuming, especially as there was no wiring diagram for the laser head, and many of the wires to be replaced had burned through.

The high voltage from the water-cooled cathode and thyatron in the laser head was carried through an extensive portion of the water lines due to the finite conductivity of the water. These lines were very close to the ground chassis, and shorts between the chassis and the water line produced leaks in the water line inside the laser head. The conductivity of the water was traced to iron in the heat-exchanger bonnets, so the bonnets were replaced with bronze bonnets, and more electrical insulation was added in the laser head. This greatly reduced the frequency of shorts in the laser head.

At the end of the program, the original laser was replaced with an improved laser possessing an output power of 20 W, with a design repetition rate of 6 kHz and a pulse energy at 510 nm of over 2 mJ. The use of this laser greatly reduced downtime and provided enough light for movies with good exposure at pressures up to 500 psi.

ANCILLARY WORK

Film Processing

Films were processed in-house to provide for good quality control in film development and excellent turnaround time, as well as some overall cost savings. A Cramer 805 processor, which can develop both 16- and 35-mm film, was used, although only 16-mm films were taken. Extensive maintenance is needed to keep this processor running properly.

A variety of films and developers were used depending on the desirability of contrast versus resolution in a given movie. A few general comments can be made about these films. Coarse-grain films require less light for exposure, and yield a high-contrast product. High-contrast films have good visual clarity, which is readily discernable by the viewer, and they project well in a motion picture projector. However, the MTF of large-grain films is poor, and fine details at unity magnification are lost with such films. Moreover, it is difficult to discriminate against flame brightness with these highly sensitive films. Better immunity to flame brightness and an improved MTF can be obtained using fine-grained films.

The resolutions of a given type of film is related to the grain size of the film. Fine-grain films (e.g., Kodak Technical Pan or Shellburst 2476) yield a high resolution, but are slow, i.e., they require more light exposure for a given level of development. The resolution limit of a film is given by the number of line pairs per mm that can be resolved. The greater the number of line pairs/mm, the better the resolution of a given type of film. In theory, a film with a resolution of 100 line pairs/mm can discern, or resolve, a $5\mu\text{m}$ object at unity magnification. In practice, the actual resolution will be significantly poorer than this, due to a reduced contrast of the object photographed.

Kodak RAR 2496 film with a resolution of 50 line pairs/mm ($10\mu\text{m}$ resolution) and RAR 2479 film with a resolution of 100 line pairs/mm ($5\mu\text{m}$ resolution) with D-19 developer, shellburst 2476 film with 160 line pairs/mm resolution ($3\mu\text{m}$ resolution) using both D-19 developer and D-76 developer, and Technical Pan 2415 film with 400 line pairs/mm resolution ($1.2\mu\text{m}$ resolution) and D-76 developer were used. The resolution of these films was reduced by about a factor of three for low-contrast subjects. Movies made with the RAR 2479 film gave a pleasing visual clarity and $25\mu\text{m}$ resolution at unity magnification. The shellburst 2476 with 200 line pairs/mm resolution was our standard film. It was used at both unity magnifications using D-19 developer and 2X demagnification using D-76 developer. Discrimination against the flames of aluminized propellants at pressures above 200 psi was obtained using Technical Pan film and D-76 developer.

The film processing at UDRI is superior to that of professional developers to whom film was sent on trial. The early movies were made as negatives. Detail was not good in early commercial positive reproductions of our movies, since the vendor who made the positive films used a coarse-grained, high-contrast film. In the later phase of the work we located a film processor who could make positive prints of our high-resolution movies. Kodak Technical Pan film was used to make enlargements. Experiments were made with a wide matrix of f stops and exposure times. The developer and enlarging lenses were also varied. It was concluded that HC110 dilution F at 68° F is the best developer for detailed enlargements using Technical Pan film. However, high-detail, low-contrast (soft) originals do not reproduce well with standard equipment. In fact, the high-contrast, low-resolution film used in the initial check-out experiments has given the best enlargements.

Inhibitor Development

Untreated solid rocket propellant has a natural tendency to burn along all freely exposed surfaces and consequently, a strand forms a pointed surface during deflagration. This "flashing" produces a pointed surface which is unsuitable for photographic experiments. Because of the limits in the photographic equipment, the desired burning surface for the experiments was a completely flat plane, parallel with the camera lens.

Strand experiments using a servopositioner are difficult to perform without a suitable inhibitor. If the inhibitor burns too rapidly, the strand profile will convert to a cone and most of the surface will be below the correct height. In particular, in photographic experiments most of the surface will be out of focus. If it burns too slowly and leaves large flakes in its residue, it will interfere with the servopositioning beam. If it smokes, the smoke will tend to mask both the servobeam and any optics that may be used in the experiment.

The relative effectiveness of traditional inhibitors was studied. One common method of inhibition currently being used in strand experiments is simply to leach the propellant with water. If leaching is done directly before deflagration, the water does inhibit burning down the sides of the strand to a relatively high degree. However, if the water is applied more than a few minutes before deflagration, its inhibitive properties are reduced greatly. Therefore it would not be applicable to any experiments where the propellant needs to be prepared long before deflagration is initiated. Also, water does not have the capability of forcing the propellant to burn at a specific angle due to different coating thickness on different sides of the propellant. Silicone grease did not fully prevent the sides from burning. In addition, it released considerable smoke. The thickness of application of the grease did not affect its performance. Sodium silicate left too much residue, or char. A

number of other commonly available materials, including lacquer and teflon, were tested with unsatisfactory results (See Figure 19).

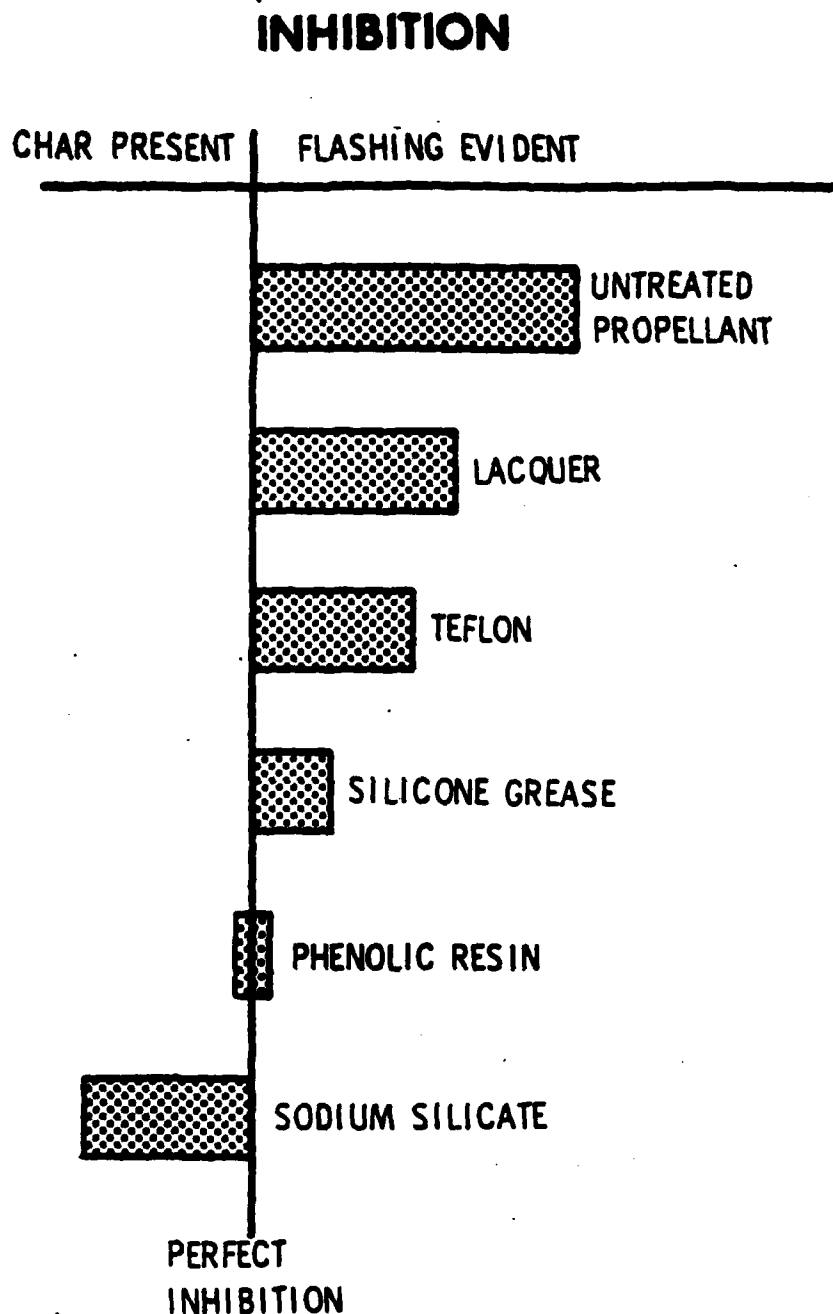


Figure 19. Qualitative Performance of Commonly Used Inhibitors for Strand Experiments.

Due to the lack of a suitable inhibitor, a smokeless, nonflaking inhibitor was developed with a burning rate that matched that of the propellant. (Ref. 22) Although this inhibitor may well have potential for use in rocket motors using smokeless propellants, its most immediate application is in strand experiments in pressure bombs in which smoking and flaking are undesirable.

Testing of alternative inhibitors has shown that a phenol-formaldehyde polymer works very well as an inhibitor on propellant strands, provided that it is properly prepared with an appropriate solvent. This phenol-formaldehyde polymer is in a partially reacted, thermo-plastic state (Figure 20). It is applied to all free surfaces of the solid rocket propellant,

CROSSLINKED PHENOLIC RESIN

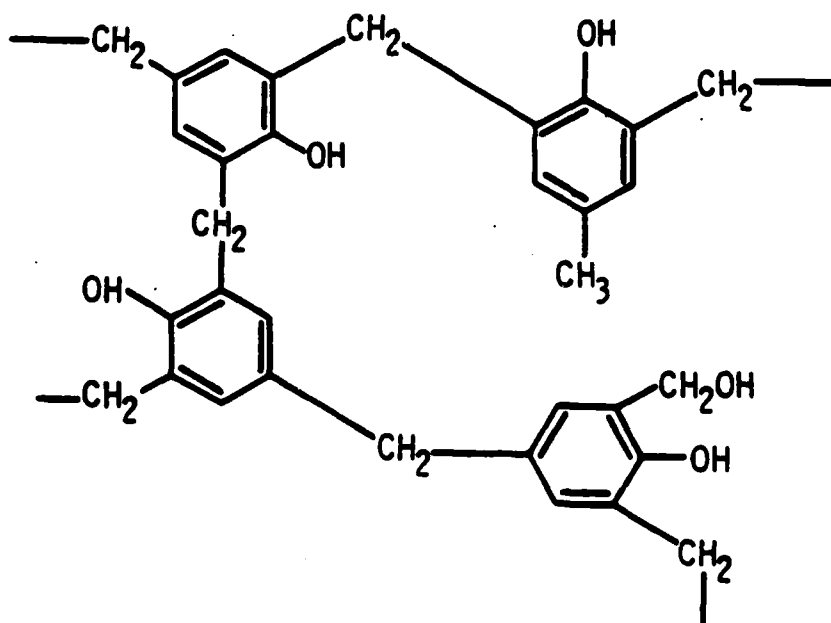


Figure 20. Chemical Structure of Phenolic Resin Copolymer Unit.

excluding the desired burning surface. The polymer will prevent the deflagration process from spreading to all free surfaces on the propellant, achieving greater control over the burning propellant. If the concentration of the inhibitor layer is

correct and the inhibitor thickness is in an appropriate range, the polymer will also burn away at the same rate as the propellant. In this case, there is no shell formation or intrusive residue left behind.

Once the polymer was established as having the most promising performance, further tests were performed to optimize the application procedure. The optimum concentration for the inhibitor coating of phenol in acetone depends on the operating pressure. An example of results for low-pressure operation is shown in Figure 21. It is expected that the optimum concentration will be different for propellants of varying formulations. Experiments were also undertaken to find the most appropriate solvent; acetone yielded a product with the most consistent results. Tests with 1000 weight polyethelene glycol (PEG) as an additive showed that more than 0.2 g/ml of PEG added to the phenol solution will cause flaking.

The initial results obtained with his inhibitor are very encouraging, but further work is needed to obtain a no-smoke, no-flake product of general interest in the solid-propellant combustion community. Additives are needed to increase the burning rate to match high-regression-rate conditions. Work should also be done to improve quality control, which is primarily limited by long (6-hr) drying times. Quality control could be improved with oven drying; both conventional and microwave ovens are possibilities for this process. A vat should be designed to control the length of the coating application time. This quality assurance would aid the progress of both research-level strand experiments and any widespread use in the solid propellant community. Additives are needed to increase the flexibility of the coating. Possibilities for enhancing flexibility are clean-burning cellulose fibers or various rubber-based compounds. The present formulation was developed for work at low (50-200 psi) pressures. Formulations for work at higher (300-1000 psi) pressures can easily be developed.

OPTICAL CORRELATOR

Much of the quantitative data needed for a statistical description of propellant combustion can be expressed in terms of correlation functions and probability density functions. This requires the automatic processing and analysis of a large number of frame sequences. It also requires high-quality films of excellent resolution and a thorough characterization of the propellants and the burn conditions.

For years, motion pictures have been extremely useful for obtaining information about the motion and behavior of a field such as the flowfields in a wind tunnel or the behavior of a turbulent flame in a combustion process. However, these movies have, for the most part, been limited to providing the qualitative understanding of the phenomena under study. Because

INHIBITION

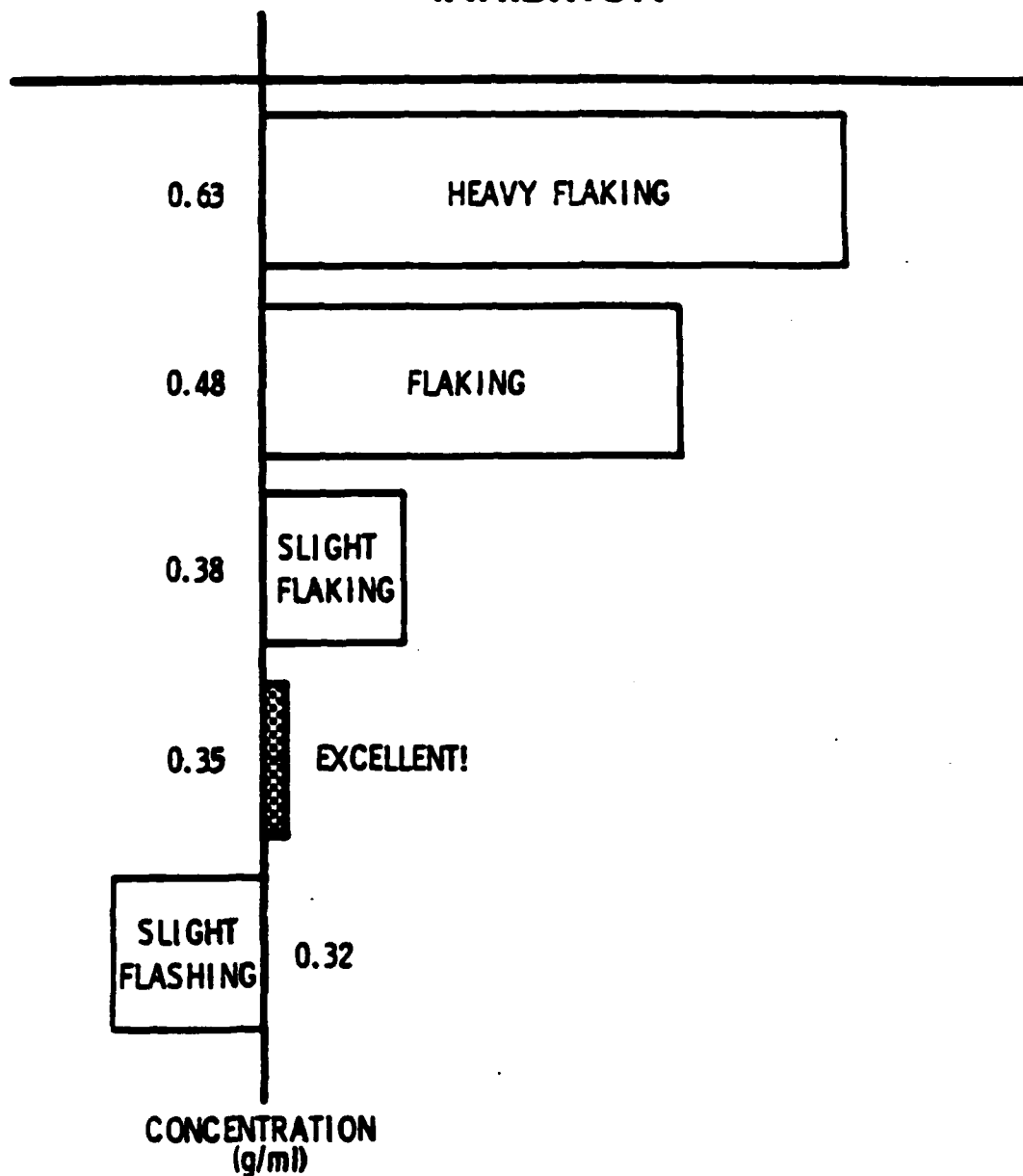


Figure 21. Qualitative Behavior of Polymer Inhibitor vs. Solution Concentration of Resinox #736.

a single picture is so rich in detailed information, reduction of the data in a movie tends to overwhelm the capacity of the digital computer. Therefore, there has long been an unmet need for a means of reducing images of essentially quasi-random fields to quantitative data.

We have demonstrated that the required automated statistical data analysis is possible using optical data processing. (Ref. 37) A successful application of this technique demands images that compromise a large number ($> 10^5$) of pixels. In the case of propellant deflagration this implies 6-mm-x-6-mm areas of the burning strand surface. This specification is due to the need to accumulate sufficient statistics, the desirability of determining long-range correlations, if any, and the logic of obtaining a realistic environment for the particles under study. The above considerations indicate that movies of the leading edge of a flame and/or of a limited field-of-view are unsatisfactory; a large field-of-view looking through the flame is desired.

A simple optical correlator has been built, demonstrated, and proven useful in addressing the above needs. This instrument has provided hard quantitative data to support our qualitative observations.

Concept

Among the types of sophisticated functions used to reduce partially random variables commonly in use are correlation functions and power or spectral density functions. The device described here provides a good quantitative description of the correlation function of a field. The advantages of the optical correlator system are that it is economical and very fast, especially in the data reduction of photographs or movies. It gives both auto- and cross-correlation, in terms of location and time. With a simple computer algorithm auto- and cross-power spectral data densities can be obtained from the correlation functions. The correlator is a simple analog system which uses a series of lenses to perform optical operations on transparencies of the images to be processed. In short, it is a single-purpose analog device which has the advantages of speed and parallel processing, as well as economy.

No viable means of obtaining quantitative data from movies of the deflagration of surfaces such as solid rocket propellant has been known to exist. Some digital computer systems have been developed for the analysis of pictures. However, because digital systems must process data serially, and because they can only handle digital data, they are slow and essentially inappropriate for the task in question. In particular, these machines must first transfer the analog information provided on the film to a detailed store of digital information. The amount of detail in a single picture is vast; it can easily incorporate a million pixels, so the memory store for thousands of frames from a motion picture is indeed enormous. To obtain a simple linear transform integral, such as the correlation distance between points, we may have to perform 10^6 or more operations.

Image analysis can be accomplished by digital data processing. A digital approach requires point-by-point analog-to-digital conversion and serial operations. To analyze a frame from a movie, we must convert the light output we get from a photograph into digital numbers, store them, and then repeat this process at least a million times to cover the entire frame. This requires sophisticated equipment to perform the A/D conversion, and a large computer memory for data storage. In addition, software is required to control the serial operations and perform simple integrals. Consequently a digital approach is a prohibitive operation. (Ref. 38)

For the above reasons, an alternative approach, analog optical data processing, was selected. It must be emphasized that optical data processing examines an entire image at once, i.e., it has the capability of performing parallel data processing. This stems from the ability to map simultaneously a single two-dimensional data field onto a second field. It is important to note that such an optical system has two spatial degrees of freedom, in contrast with a digital system whose single independent variable is time. An optical system also has good speed potential; the simultaneous analog multiplications take place as fast as the response time of the photodetector. In summary, optical data processing systems are powerful, fast, and economical. (Ref. 39)

The simplest way to perform an incoherent optical operation is to make use of the ability of a lens to form images. (Ref. 41) The principle of this processing is straightforward. If a transparency with transmittance $f(x,y)$ is imaged onto another transparency with transmittance $h(x,y)$, the resultant transmitted intensity is the product of the two transmittances, i.e., $f(x,y)h(x,y)$. If a collection lens and a photodetector integrate the resultant intensity product, an output of the form

$$I = \int \int f(x,y)h(x,y) dx dy \quad (13)$$

is obtained.

This operation can be approached by two techniques. In the first technique, a lens images the uniform incoherent source into two transparencies which are in contact. The intensity product formed by the two transparencies is integrated by the second lens and a photodetector; the output is given by Equation (13). (Ref. 21) This technique has a mechanical difficulty if one of the two transparencies is moved because of the direct contact between the two transparencies. Therefore, it is more convenient to separate them (Figure 22).

Many one-dimensional and two-dimensional linear transformations can be achieved by moving the first transparency, the second transparency, the imaging lens, or any combination of those. These include convolutions, correlations, power spectra,

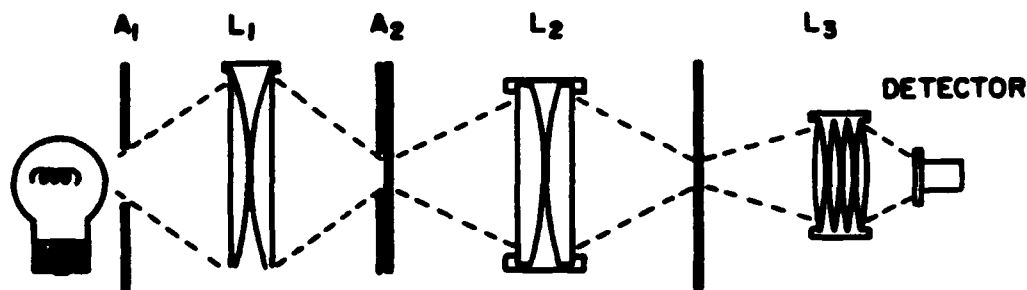


Figure 22. Optical Correlator. This simple layout provides parallel data processing and integration. Apertures are designated by A, lenses by L, and transparencies by T.

filtering, and other useful linear transformations. In spatial scanning systems the integration takes place over spatial variables, as seen in Equation (13). When the second transparency is translated by an amount of x_0 , the photodetector output yields a one-dimensional cross-correlation of the form (Ref. 41)

$$I(x_0) = \int f(x)h(x_0 - x)dx. \quad (14)$$

Practical Considerations and Limitations

It is essential to ensure that all the optical components, including the light source, lenses, and photodetector are centered on the optical axis. This minimizes off-axis aberrations and vignetting. The first transparency must be illuminated uniformly. Because of the problem in uniformly illuminating the first transparency within the translating distance, the first was fixed at the most uniformly illuminated spot, and the second transparency was moved.

The most difficult problem was aligning the image of the first transparency on the second one, due to the nature of the propellant image. The shape of the propellant during combustion does not have straight edges or clear corners that can be used for alignment. A three-axis system was used for image alignment. The z-axis translation stage fixed the magnification obtained from the imaging lens: Two translation stages gave the x-y translation portions. The third stage rotated the transparency in the x-y plane. The use of these three stages eased the image alignment. Final alignment required judgment on the part of the experimenter.

Because the transparency darkness was not the same across the image of the propellant strand, a condition of maximum output

light did not necessarily indicate that the two transparencies were properly aligned. Minimizing background effects required a dark background and several bright features.

Results were significantly affected by the contrast of the transparency. Work began with a fine-grain positive film transparency (Figure 23). This type of film has a continuous range of opacity and the resultant data were difficult to



Figure 23. Untreated Photograph of Combusting Surface. The lack of contrast on the surface impairs the signal-to-noise ration.

interpret (Figure 24). Therefore, films were processed by using a very high contrast film, resulting in pure black and white tones (Figure 25). This type of positive film enhanced the signal from the bright intermediate-sized features in the images. Sharp correlation functions were obtained from these photographs. We interpreted the widths of these correlation functions as a direct measure of the sizes of bright features on the surface (Figure 26).

Electronic noise from the dual power supply (± 15 V) and from the active elements of the circuit itself was minimized. The power supply noise was reduced by coupling the high-voltage leads of the power supply to the ground lead with two capacitors, one for the positive lead and one for the negative lead. The circuit noise was reduced by shunting a capacitor across the feedback resistor.

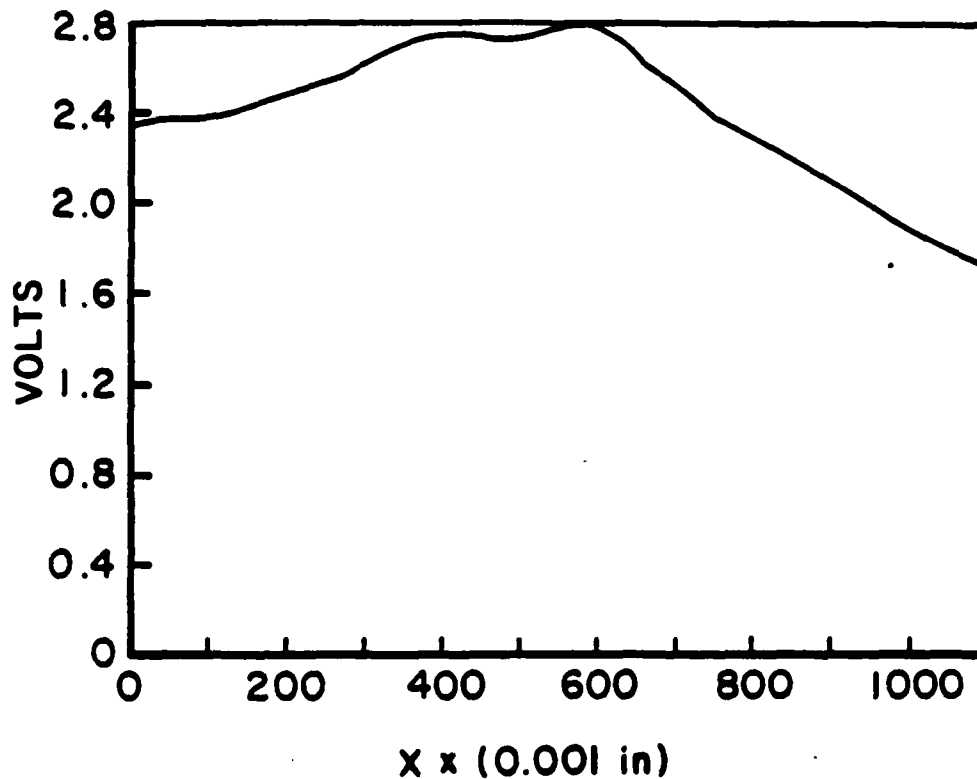


Figure 24. Correlation Function Obtained from Untreated Photograph. Long-range correlations are difficult to extract without analyzing a large number of frames.

STEREO CINEPHOTOGRAPHY

Present understanding of the details of propellant combustion is sparse and would benefit from more detailed qualitative information, as well as quantitative information. More information is needed about localized transient burning rates, their dependence on grain and binder composition and grain size distribution, and the coupling of regression rates of the various constituents in the propellant. High-speed movies have long been a very useful means of obtaining a qualitative understanding of the behavior of the combusting surfaces especially in the field of solid propellant combustion. It may be possible to analyze a series of high-speed cinematic frames to trace the local regression of the surface along trajectories normal to the local surface and not simply to record the recession of a mean plane normal to the strand axis. This objective requires movies with depth perception. One means of achieving depth perception is by stereo cinephotography.



Figure 25. High-Contrast Photograph of Combusting Surface. High-contrast processing enabled us to obtain a signal dominated by the brightest features on the surface.

Detailed front-lit stereo movies of the combustion of solid propellants have been made. (Ref. 42) It is believed that these are the first stereo movies ever made on solid-propellant combustion. Two complementary images of good quality at pressures up to 250 psi were obtained. Stereo movies at 300 and 350 psi were also made. At 350 psi problems were encountered from one camera angle with flame turbulence, although we were able to obtain pictures in focus at 300 and 350 psi.

The two viewing ports were configured at a wide (90°) angle to maximize the depth resolution obtainable. This resulted in dramatic differences in the viewing perspective. Our motivation for selecting a widely disparate viewing angle was to maximize our depth resolution. The relation between the depth resolution, ζ_d , of a stereo movie and the transverse resolution, ζ_T , of the optical system is given by

$$\zeta_d = \zeta_T / \sin \frac{1}{2} \phi$$

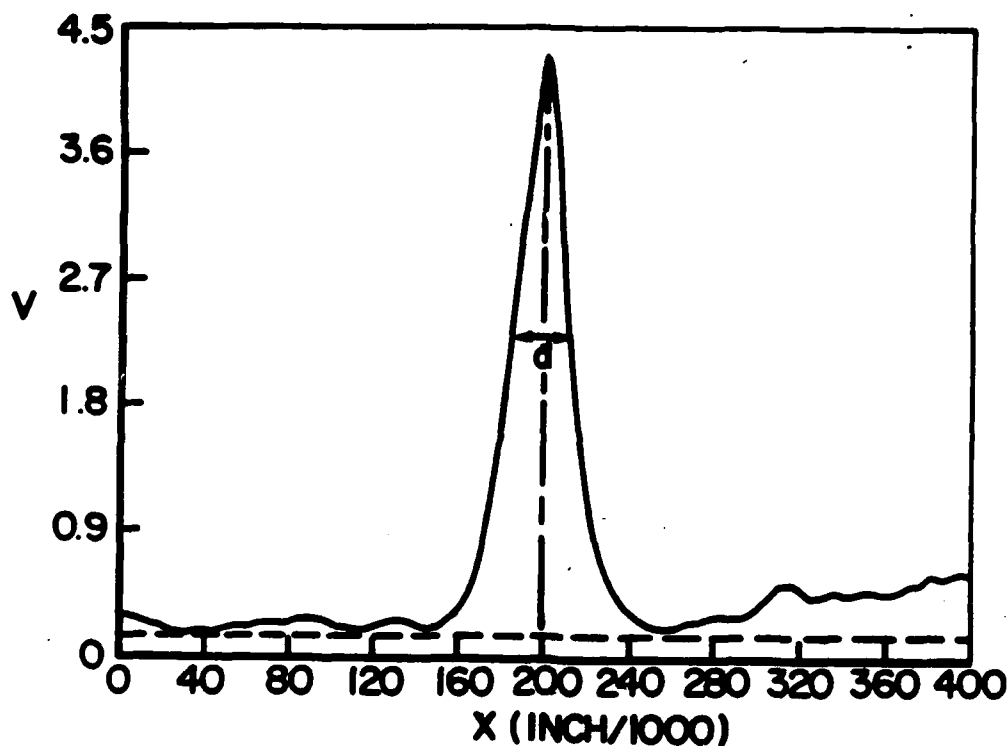


Figure 26. Correlation Function Obtained from a High-Contrast Photograph. We interpret the width of the correlation peak as a measure of the size of the bright features on the surface.

where ϕ is the angle between the two viewing ports. Since an ability to discern depth relationships is limited by the depth resolution, it is helpful to make r_d as small as possible. Consequently, with cinephotography optics of a given quality, good depth resolution can only be achieved by using a large angle between the two viewing perspectives. The objective in seeking good depth resolution was to optimize scientific understanding. A narrower stereo perspective would be more suitable for obtaining films with images that could be superimposed by an appropriately configured projector to lend a natural image to the viewer. This was not the aim of the experiment. However, since stereo feasibility with a wide viewing angle has been demonstrated, it is felt that stereo movies using a narrow viewing angle can easily be obtained.

The camera and the stereo camera optics were mounted on a single 30-in.-x-18-in.-x-0.5-in. (75-cm-x-45-cm-x-1.3-cm) aluminum plate. Brackets were made to secure this plate to a camera tripod at the desired height and angle. Mirrors directed the light from each of the two viewing ports to a second set of

mirrors, which then directed the (by now) nearly parallel light beams to a single camera lens (Figure 27).

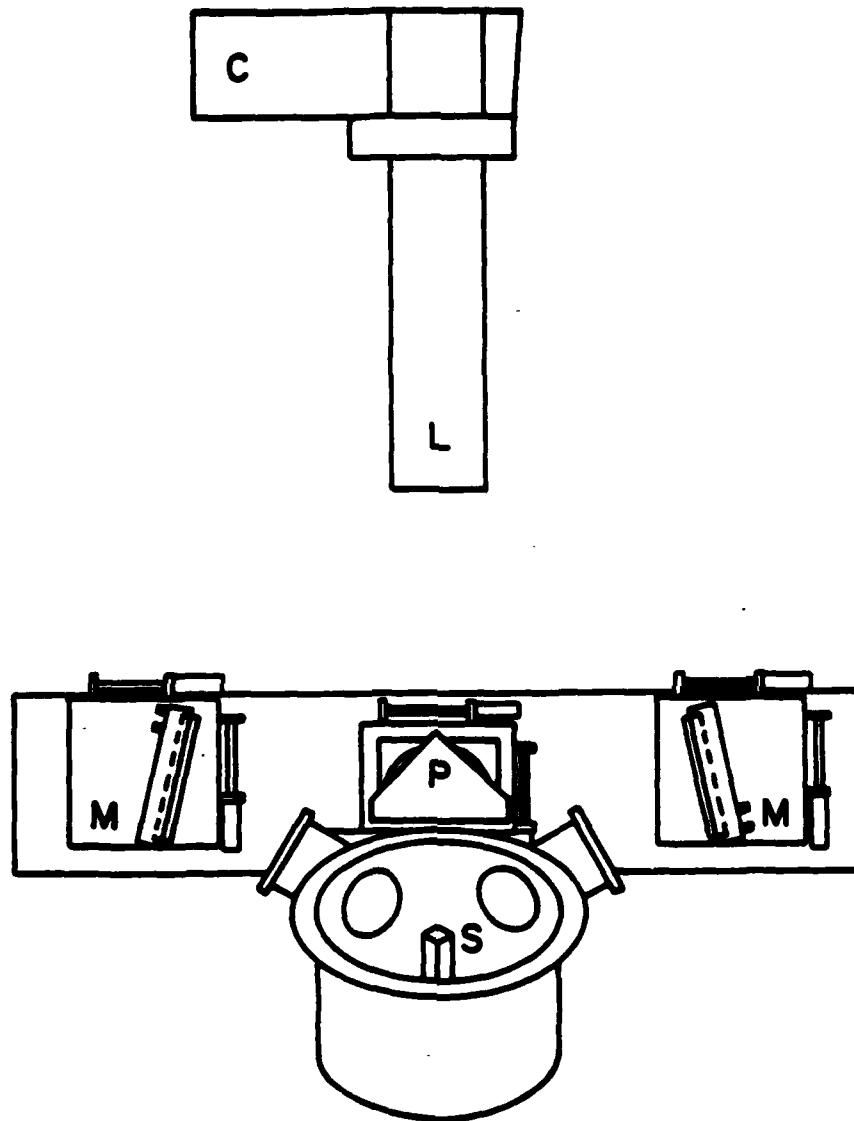


Figure 27. Stereo Optics. A mirror and prism arrangement allowed us to simultaneously record two separate images.

The viewing ports were arranged at a 45° angle with respect to the horizontal so that they looked down on the deflagrating surface of a vertically mounted strand (Figure 28). The illuminating light was brought in along a horizontal path, and

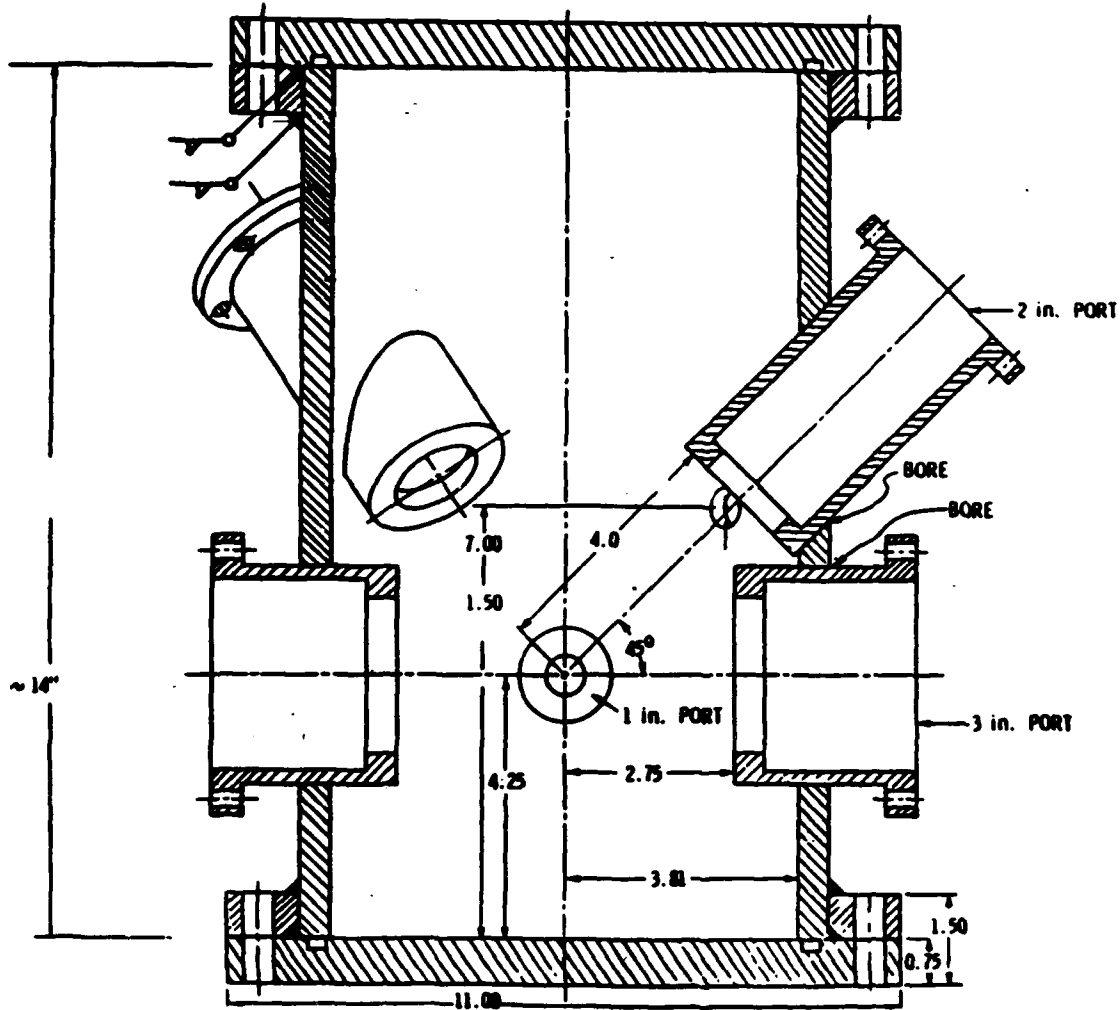


Figure 28. Side View of Window Bomb. The 45° viewing angle allowed us to survey the entire active surface of the strand.

the strand surface was cut at 45° to face the viewing ports as much as possible. (Ref. 21) The detailed movies obtained were immune to flame brightness and motion blur over a wide field-of-view at 7000 frames per second. (Ref. 36)

Our initial trials of stereo photography were troubled by differences in optical path length, vignetting between the two optical trains, and vibrations induced by the camera. The first two difficulties were overcome by very careful alignment. Vibrations were minimized by damping and clamping. The area of support contacts to the mounting plate was increased and the mounting plate was tightly clamped to the camera framework. The mounts for the mirrors and prism were secured with wedges and clamps. The camera lens was also clamped. A half-inch-thick layer of damping material was placed under the camera and the rail supporting the stereo optics. The prism directing the two images to the camera was reconfigured to an 85° angle instead of a 90° angle. This provided more flexibility in positioning the mirrors, and allowed us to locate them so as to minimize vibrations. The different perspectives of the sides of the strand were oriented in such a way that they crossed at an odd angle, resulting in what was effectively a double exposure of the strand sides with the strand surfaces. This problem was surmounted by crossing the images from the left to the right. Thus the recorded pictures are mirror images of the true object field.

A sample stereo image is shown in Figure 29. The groove in the strand face shown in this figure was cut to provide good



Figure 29. Stereo Images of Burning Propellant Surface. No fuzziness occurs due to flame brightness, motion blur, or flame turbulence.

thermal contact for the ignition wire. This groove has widened due to deflagration. The differing textures on the strand face mark the flame front. Note that no flame emission or motion blur appears in these photographs; single frames are not fuzzed out, despite a low-contrast object field. The change in perspective in the two images in Figure 29 is dramatic. Figures 30 and 31 show a similar strand, taken several frames apart during the course of filming. A close inspection of these photographs will reveal changes in the surface topography between the two frames, and a sharply varying perspective between the left and right images of a given particle.



Figure 30. Stereo Images of Burning Propellant Surface.
Surface has not yet fully ignited.

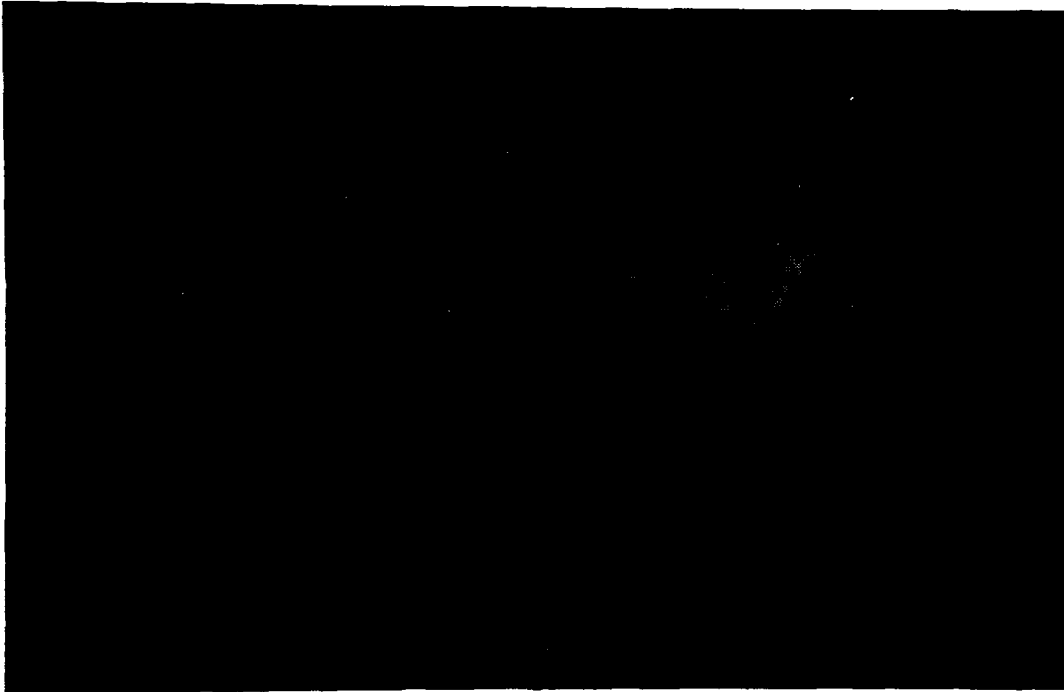


Figure 31. Stereo Images of Same Subject as Shown in Figure 29, Taken Several Frames Later. The surface is now fully ignited.

RESULTS

The experiment was successful in accomplishing most of its goals. A window bomb with plentiful optical access suitable for the experiment was designed and built. A servopositioning circuit based on an array of photodetectors was designed and demonstrated. Movies were taken on ten AP propellants at pressures of up to 500 psi. Stereo cinephotography was demonstrated. The results from this work are described below.

GENERAL PERFORMANCE

The 2.1 mJ pulse energy and 510 nm monochromatic output of the copper-vapor laser in conjunction with slow (insensitive) film and a line filter permitted flame brightness to be overcome and the surface topography within the combustion region to be seen through the flame. The intensity of the laser pulses together with their short (25 ns) pulse width allow use of the laser pulse as a shutter. Conventional cinephotography uses shutters that are tied to the film framing rate. Consequently, the motion blur induced by the movement of the film in the camera is a fixed fraction of the frame size. For a 16-mm film with a 1/100th shutter at unity magnification, this implies a minimum blur of 70 μm . A 25-ns pulse width produced a film blur of only 1 μm , even at a framing rate of 6000 frames/s. The copper-vapor laser, slow film, and line filter have been totally successful at overcoming flame brightness and motion blur; these two technical difficulties have no bearing on the quality of the films.

The movies clearly prove the ability of the pulsed laser technique to overcome difficulties associated with the inherent incandescence of the flames of individual particles and of motion blur, particularly blur produced by the motion of the film in the camera. A highly logical approach involved the use of an intense, high-energy, monochromatic, and extremely short laser pulse. Difficulties with flame brightness and motion blur simply do not occur. It is emphasized that these front-lit movies are taken across the entire field of the burning strand normal to the surface and that an ability to reach framing rates of six to seven kilohertz has already been demonstrated. Although this makes the cinephotography task difficult, these requirements are essential to understanding the response of the propellant to external high-frequency driving forces such as pressure oscillations and to finding correlations in the behavior of various particles across the surface in the presence of pressure oscillations. Furthermore, these movies were made for extended time periods. Great effort went into making movies which will obtain high resolution for a great many frames. In general, useful information during the entire course of a movie can be obtained. Resolution on the order of 15 microns is obtained, even on propellants which contain no metal. This is an especially difficult task because such propellants have no inherent contrasts on their surfaces. Furthermore, these movies

are seldom troubled by smoke from the burning propellant, even in movies on carbonized and heavily aluminized propellants. It is demonstrated that speckle due to the coherence of the light source can easily be eliminated, and good ruggedness against flame turbulence has been shown.

The above performance should be put into proper context with conventional technology. Although experiments using conventional illumination have in some instances matched any one of the above performance characteristics of these movies, it is not known that anyone has been able to achieve comparable results when all of these various performance parameters are taken together: field-of-view, duration of the movie, framing rate, and resolution, not to mention immunity to flame brightness, smoke, and the ability to resolve details on low-contrast surfaces.

AP MATRIX BEHAVIOR

A large number of movies (300) on various solid propellants, all of which have ammonium perchlorate (AP) formulation, were taken. Most of the movies were made on wide-distribution AP propellants. The particle sizes are in various proportions of 3/20/400 microns. These propellants are 87% AP and 13% HTPB binder, using both IPDI and DDI curatives.

We used a 10W early version of a commercial copper-vapor laser for the initial combustion photography experiments. Since this was really an experimental version of the product, we found it necessary to make a number of improvements on the unit. We modified the laser power supply and the head to minimize the possibility of damage due to failure in the cooling system. The Tygon water lines were replaced with nylon lines, allowing for a higher temperature and pressure margin, and a temperature-sensing interlock was installed in the power supply. Improvements in various grounds and insulators resulted in a reduction in the frequency of occurrence of laser lockup and stray timing marks. The laser head was subject to frequent high-voltage breakdowns. Part of this was an rf breakdown, due to the intense fields generated in the 100 MW breakdown discharges in the plasma tube. The fundamental frequency of this rf field was about 30 MHz. The laser head was too small, making it difficult to isolate electrically the various components crowded within it.

The high voltage from the water cooled cathode and thyatron in the laser head was carried through an extensive portion of the water lines due to the finite conductivity of the water. These lines were very close to the grounded chassis, and shorts between the chassis and the water line produced leaks in the water line inside the laser head. We traced the conductivity of the water to iron in the heat-exchanger bonnets, replaced the bonnets with bronze bonnets, and added more electrical insulation in the laser head. This greatly reduced the frequency of shorts in the laser head.

As expected with a new product, there were several maintenance problems with the initial copper-vapor laser. A fault in the thyatron driving frequency circuit caused fuses and components to blow. A transformer, a resistor/diode chain, and a driver tube blew in the driver circuit on several occasions. The large capacitors in the laser head leaked oil and exploded when the oil reached ground, spraying glass and oil around the laser head. A lead to the bleeder resistor in the head was never properly secured during installation. The lead broke free, producing a short, which set afire some oil remaining from the leakage of the main capacitors. The mylar insulation we were using then caught fire and burned out the wiring around the thyatron. We remachined the mounts for the capacitors, installed capacitors which were resistant to leaking oil, and rewired and replumbed the laser head and replaced the mylar insulation with pyrex and fiberglass insulation. Unfortunately, these repairs were very time consuming, especially as there was no wiring diagram for the laser head, and many of the wires which we replaced had burned through.

The maintenance problems with the original laser led to extensive downtime, as much as 80%, throughout its final year of use. Since we determined that a high-power level was critical to the quality of the movies obtained, especially at higher operating pressures, a new 20W laser was purchased by the University of Dayton.

Upon installation of the 20W copper vapor laser, it became possible to take movies of good quality at pressures above 200 psi. The highest pressure at which good films were achieved was 465 psi. These movies definitely established both the strengths and limitations of the experiment as well as the unexpected nature of the deflagration of wide-distribution propellants, which we will now discuss.

Deflagration Behavior

Most of the movies featured the ER series of propellants provided by AFAL at the beginning of the initial program. The ME series showed similar behavior. The most striking features of the deflagration of these propellants was that the ignited surfaces instantly became wet and the intermediate-sized particles went into rapid oscillations. Most movies were made of the ignition of a strand. Quarter-inch strands were oriented in a vertical position. Usually the top end would be cut at 45° and the strand would be ignited at the top end of the cut. Often a straight cut would be made instead. In the case of a straight cut the uninhibited surface was barely visible, but the profile of the burning surface would be accentuated. As the flame front progressed down the face of a 45° cut, the sharp boundary between the ignited and unignited surfaces was clearly evident, due not to presence of any flame but due to the smooth, wet surface and lack of sharp edges on particles within the flame zone, as well

in which they scatter the strobe illumination. The AP particles are semitranslucent. Apparently, interference effects occur between light scattered from the front and back surfaces of the small particles and the tips of the large particles, so that they reflect light with high efficiency. By contrast, much of the light reaching the ignited inhibitor is absorbed in the material itself, so that it is relatively dark. Small portions of the surfaces of the large particles that are oriented in the appropriate direction cause specular reflections of the laser light toward the camera optics. These areas also show up brightly in the films. As ripples move across the large AP particles these bright areas also move. This enables the ripples to be discerned.

A few movies were made using ballistic propellants at 15 psi. In those movies, the large AP particles showed no motion, whereas intermediate-sized particles oscillated rapidly upon ignition, just as in the case of the wide distribution propellants. This shows that whereas the deflagration behavior is a function of the propellant formulation and the operating pressure, many of the observations made on the wide distribution propellants may carry over to other nonmetalized propellants.

As the operating pressure increased above 100 psi many of the propellants began to smoke. Smoking took two forms. In the first case smoke rose in persistent, localized plumes from specific regions of the surface. As the operating pressure increased, the number of these plumes increased. The plumes rose in chimneys well above (>1 cm) the surface. The sites from which the plumes originated were always in the binder between the large particles and tended to be towards the center of the strand, where the temperature is higher. Another reason for associating flame temperature with the occurrence of the plumes is that there was often a delay between ignition and the occurrence of the plumes, as well as the correlation between the incidence of plumes and operating pressure.

The second type of smoke formation was a blanket of smoke that hugged the surface, especially in depressions. The behavior of this smoke film on the burning surface was reminiscent of fog. The smoke layer gives a soft cottony appearance to the surface, and thickens with increased operating pressure. As the smoke blanket thickens, only the elevated tips of the large particles remain visible, so that the only oscillations that can be seen are the ripples at the tips of the big particles, the oscillations of intermediate sized particles at the edge of the strand, and long wavelength undulations of the surface. As in the case of the smoke tufts, there is a delay between ignition and the formation of the smoke film.

Since the smoke is confined to a thin region near the surface it seems that some of the inhibitor must finish combustion in the form of a suspension of very fine particles just above the surface. Clearly the smoke film can easily follow

in which they scatter the strobe illumination. The AP particles are semitranslucent. Apparently, interference effects occur between light scattered from the front and back surfaces of the small particles and the tips of the large particles, so that they reflect light with high efficiency. By contrast, much of the light reaching the ignited inhibitor is absorbed in the material itself, so that it is relatively dark. Small portions of the surfaces of the large particles that are oriented in the appropriate direction cause specular reflections of the laser light toward the camera optics. These areas also show up brightly in the films. As ripples move across the large AP particles these bright areas also move. This enables the ripples to be discerned.

A few movies were made using ballistic propellants at 15 psi. In those movies, the large AP particles showed no motion, whereas intermediate-sized particles oscillated rapidly upon ignition, just as in the case of the wide distribution propellants. This shows that whereas the deflagration behavior is a function of the propellant formulation and the operating pressure, many of the observations made on the wide distribution propellants may carry over to other nonmetalized propellants.

As the operating pressure increased above 100 psi many of the propellants began to smoke. Smoking took two forms. In the first case smoke rose in persistent, localized plumes from specific regions of the surface. As the operating pressure increased, the number of these plumes increased. The plumes rose in chimneys well above (>1 cm) the surface. The sites from which the plumes originated were always in the binder between the large particles and tended to be towards the center of the strand, where the temperature is higher. Another reason for associating flame temperature with the occurrence of the plumes is that there was often a delay between ignition and the occurrence of the plumes, as well as the correlation between the incidence of plumes and operating pressure.

The second type of smoke formation was a blanket of smoke that hugged the surface, especially in depressions. The behavior of this smoke film on the burning surface was reminiscent of fog. The smoke layer gives a soft cottony appearance to the surface, and thickens with increased operating pressure. As the smoke blanket thickens, only the elevated tips of the large particles remain visible, so that the only oscillations that can be seen are the ripples at the tips of the big particles, the oscillations of intermediate sized particles at the edge of the strand, and long wavelength undulations of the surface. As in the case of the smoke tufts, there is a delay between ignition and the formation of the smoke film.

Since the smoke is confined to a thin region near the surface it seems that some of the inhibitor must finish combustion in the form of a suspension of very fine particles just above the surface. Clearly the smoke film can easily follow

the oscillations of the surrounding gas. The oscillating intermediate-sized particles and the ripples on the surface of the large particles are highly responsive as well. Thus the surfaces of the wide distribution propellants appear to couple strongly to oscillations in the gas phase.

The smooth rounded domes of the large AP particles rising above the inhibitor and the wet texture of the surfaces are clearly evident in the 15-200 psi movies. As the pressure increases, the large AP particles compress against the surface, an indication that they are becoming soft. This flattening results in an increase in the size of the bright reflecting areas on the particles. The growth in mean diameter with pressure of these particles increases sharply at 150 psi (see Figure 32),

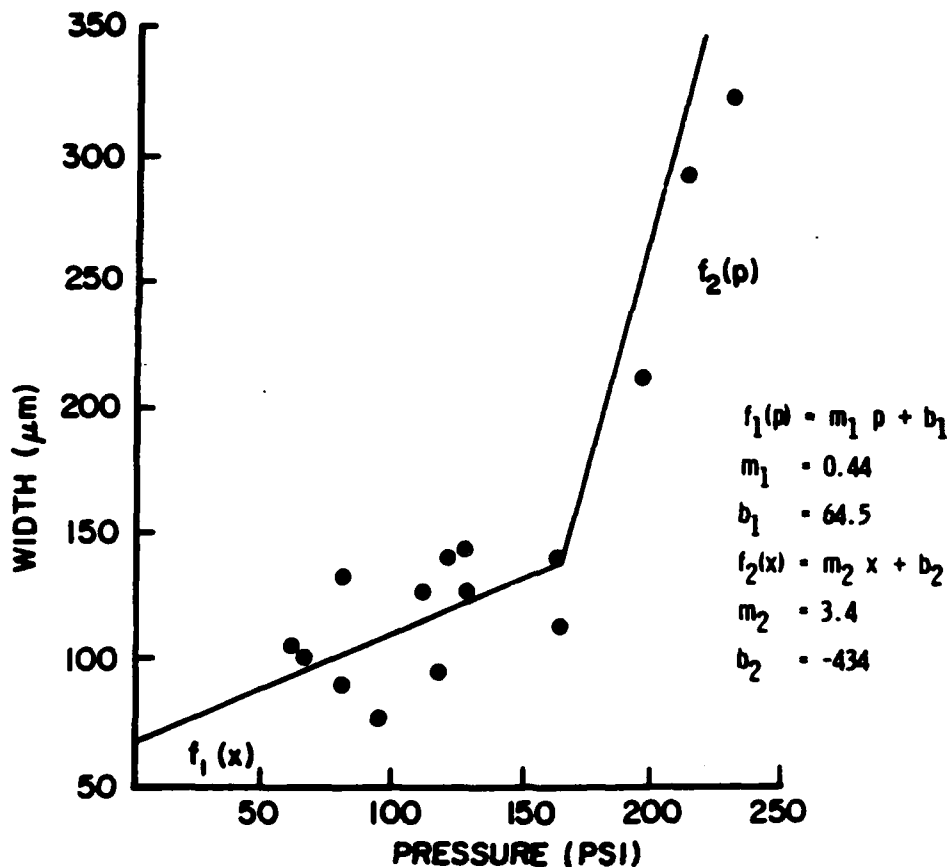


Figure 32. Best Fit to Correlation-Width Data.

indicating that the internal rigidity of the AP particles drops at a temperature associated with this operating pressure.

Since flame turbulence increases rapidly with operating pressure and since oscillation of particles has not been reported before, the true nature of the apparent oscillations may be questioned. The author is confident of his analysis for the following reasons:

- The stainless steel pointer and reference wires in the flame gave no appearance of oscillation, although small particles attached to them oscillated.
- In some ignition movies, a gust of flame would occasionally sweep over unignited propellants. The effect of flame turbulence could then be readily distinguished. The effect is to obscure fine details, not to simulate oscillations. The appearance of unignited particles, seen through a sheet of turbulent flame, is entirely different from the appearance of ignited propellant.
- The boundary between the large particle and the binder is sharp and clear in the 15-200 psi movies. This boundary remains distinct and does not give any appearance of movement, whereas intermediate-sized particles nearby oscillate rapidly.
- Oscillatory motion can be seen at the edges of a strand and at the flame front boundary, conditions which minimize the effects of flame turbulence.
- No oscillations are seen on metalized propellants. This shows that the effect depends on the propellant properties and not on the existence of flame turbulence by itself.
- Rippling of the ignited surface shows up in the profile movies, where flame turbulence is again at a minimum. The long wavelength oscillations give further evidence that the burning surface is soft.

These observations clearly have strong implications for models of the behavior of burning solid propellant surfaces. The raised features, which are free to oscillate at moderate frequencies, are not accounted for in conventional theories, which treat the surface as smooth and which treat pressure coupling as occurring through thermal waves at the surface. It is evident that the particles can couple to external pressure oscillations. The smooth surfaces, which we see once ignition has occurred, indicate that the surfaces are, in fact, molten.

It is highly probably that the very fine-scale particles have melted or tend to melt immediately as they approach the surface. It seems that models of surface deflagration based on the initial ordering of particles in the grain of the propellant are faced with serious difficulties.

The movies obtained in this earlier research show that HSLP can not only provide much of the qualitative capability needed to study the details of propellant combustion, but can also yield a wealth of quantitative data and reveal unanticipated behavior. This capability should be extended to improve performance.

CORRELATOR RESULTS

Our optical correlator was used to analyze selected frames from the movies. Fifteen different movie frames were analyzed at different pressures (see Table 1). It was found that the characteristic sizes of bright features at the surface vary with

Table 1.
Size of Bright Features vs. Operating Pressure.

Pressure (PSI)	Propellant		Width μm	Film #	Frame #
	Grain #	Large Grain #			
62	7	38	104	LS93	28849
63	15	47	102	R12	35840
80	7	38	92	R19	35568
80	7	38	134	R19	35546
95	12	38	78	LS90	70060
112	17	44	128	R24	78090
116	10	47	97	R25	75736
121	11	30	142	R23	90363
127	13	41	145	LS62	27396
127	17	44	128	LS63	90472
163	15	47	119	R26	70611
164	9	44	142	R27	76607
195	12	38	215	LS34	83599
211	11	30	208	LS35	73626
228	9	44	326	R29	97390

pressure, but not with the particle mix of the propellant. A best fit to the data was made using three different curves and a standard χ^2 routine. (Ref. 43) The first curve was an exponential function in the form

$$f(p) = A + B e^{p/c} \quad (15)$$

The parameters giving the best fit to the data were $A = 59.27$, $B = 15.87$, and $C = 90.97$ (Figure 33). The reduced χ^2 was 0.43, indicating a 96% probability that the data were nonrandom.

The second curve was a quadratic function in the form

$$f(p) = A + Bp + Cp^2 \quad (16)$$

A χ^2 fit yielded the following optimized parameters: $A_2 = 70.0$, $B = 0.12$, and $C = 2.46 \times 10^{-3}$ (Figure 34). The reduced χ^2 of 0.47 gave a 94% probability that the data were nonrandom.

The third curve was a broken line of the form $f_1(p)$ and $f_2(p)$, where

$$f_1(p) = m_1 p + b_1 \quad (17)$$

and

$$f_2(p) = m_2 p + b_2 \quad (18)$$

In Equations (17) and (18), m_1 and m_2 are respectively the slope for the first line and the second line, b_1 is the y-intercept of $f_1(x)$, and b_2 is the y-intercept of $f_2(x)$. A χ^2 fit gave $m_1 = 0.144$, $b_1 = 64.5$, $m_2 = 3.4$, and $b_2 = 434$ (Figure 32). The reduced χ^2 of 0.36 indicated a 98% probability that the data were nonrandom. The conclusion is that the best fit for the data set is given by the broken line.

One frame in a movie was compared with succeeding frames to obtain the temporal as well as the spatial correlation. The plot of the highest response of each frame versus the frame-time order was also expected to be in the shape of an exponential decay. This would result from the decrease in the size of particles as they burned. The measured curve turned out to be a damped cosine function (Figure 35). This implies that an oscillation is associated with the combustion process. These data are the first quantitative verification of this result. To make the best curve fit for these data points, a standard χ^2 fitting routine was again used. The specified function to which we fit the data points was a damped cosine curve:

$$f(t) = A[B + \cos \omega t] e^{-\nu t}, \quad (19)$$

where A was the initial peak amplitude, B gave a dc offset to the oscillation amplitude, ω was the oscillation frequency, and ν was

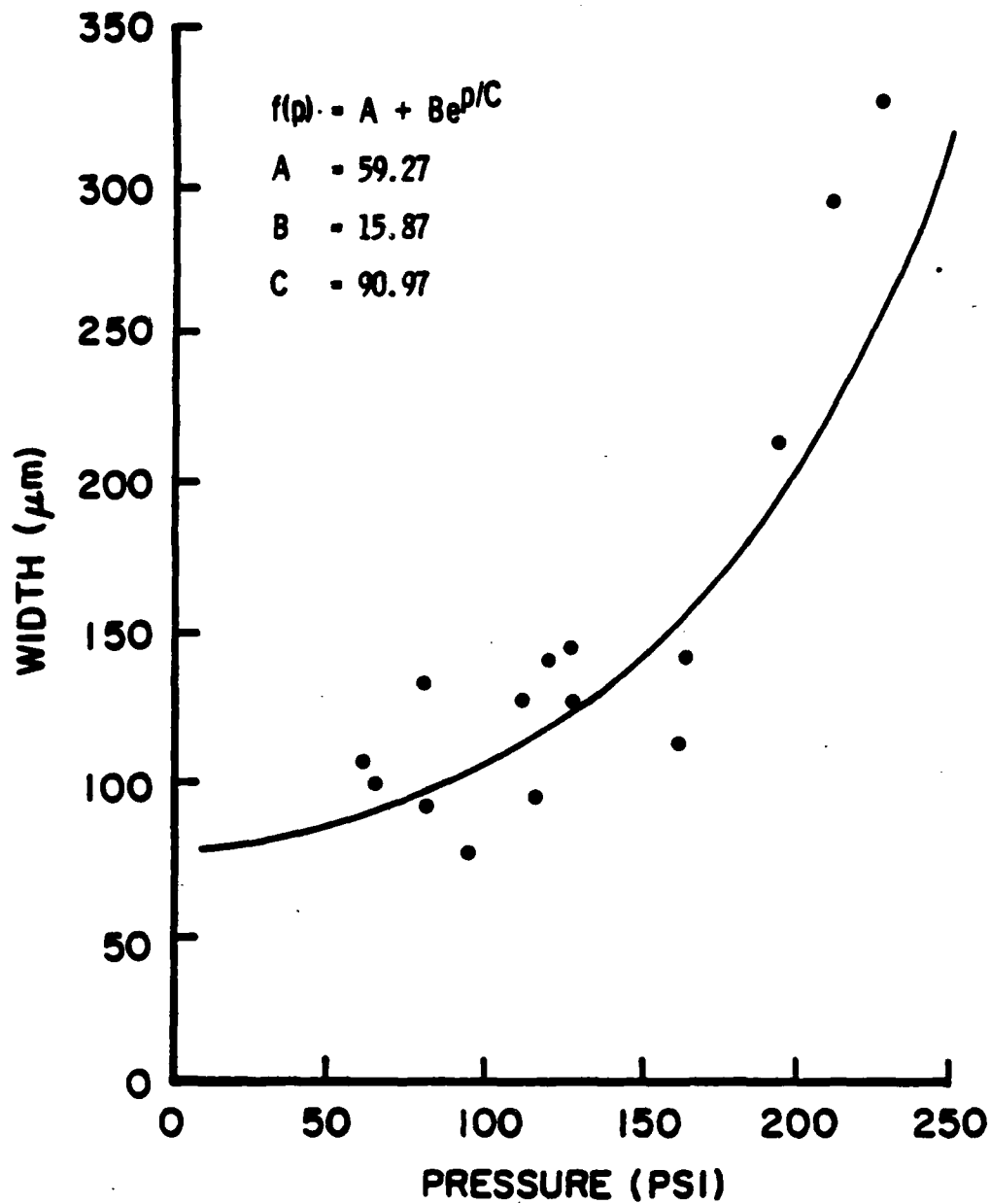


Figure 33. Exponential Fit to Size vs. Pressure Data.

the damping rate. The optimized parameters₂ were: $A = 1.4$, $B = 1.31$, $F = 0.118$, and $\nu = 18.8$. A reduced χ^2 of 0.38 was also obtained, giving a 97% probability that the data were nonrandom.

A similar analysis was used to measure the trend in the widths of the correlation functions vs. time (Figure 36).

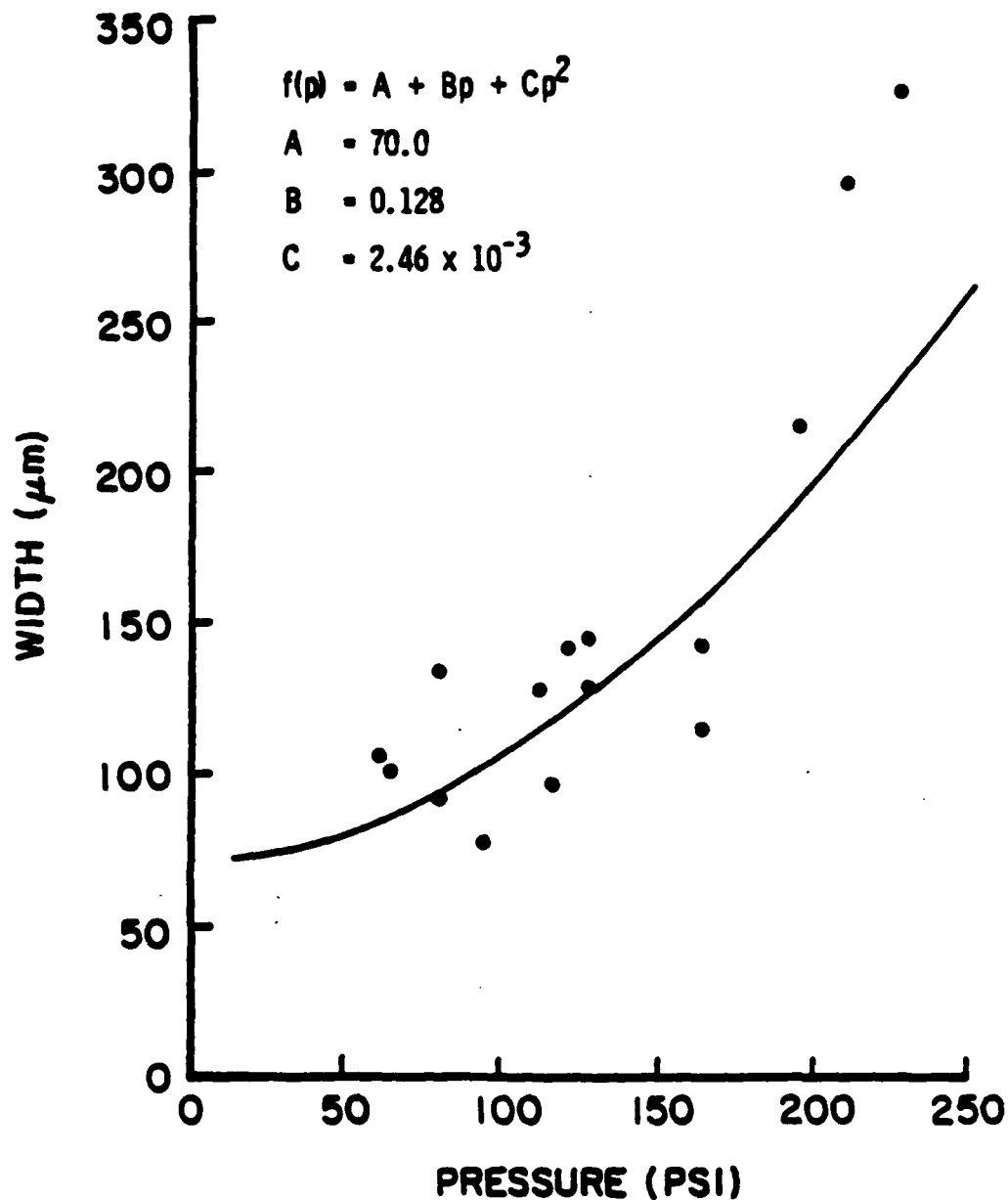


Figure 34. Quadratic Fit to Size vs. Pressure Data.

Although there is a good deal of scatter in these data, it does appear that the widths of the cross-correlation functions increase as the time between frames increases. This suggests movement in the apparent location of the bright features at the surface. A standard linear-regression routine was used to obtain

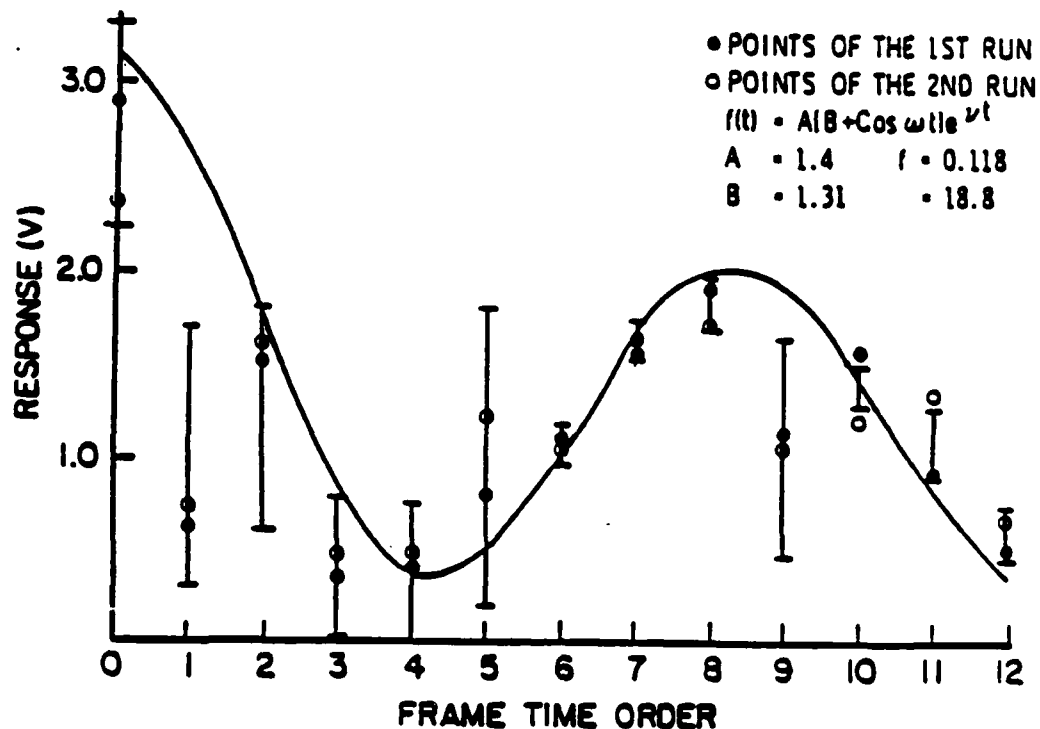


Figure 35. Time Dependence of Correlation Peak Height.

a fit. This routine made a least-square fit to the data with a straight line, i.e.,

$$f(t) = mt + b, \quad (20)$$

where m was the slope, and b was the y-intercept of the fitted line. With different weightings for the various y-values represented by the bars on the plot, the routine's output was $m = 4.68$ and $b = 126.8$. The linear correlation coefficient was 0.74. The probability that the data points were not correlated was 0.4%.

ADDITIONAL OBSERVATIONS

Movies were undertaken without using the line filter on the camera optics to explore the possibility of examining particle ignition. With shellburst film, streaks from flames occurred across the frames, but it was not possible to associate them with a given particle. Due to flame brightness, most of these films were of unacceptable quality. These streaks did not occur at low pressure using the slower Technical Pan film. It was even possible to film aluminized propellants successfully without a line filter at pressures below 100 psi using this film. Some control on the amount of flame emission recorded could be achieved by varying the line width of the line filter and the speed of the film.

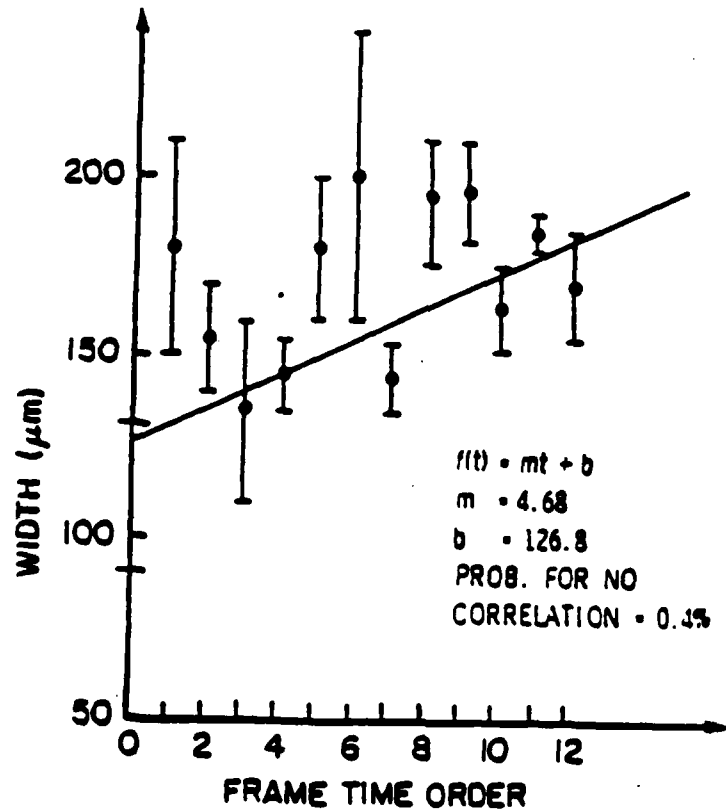


Figure 36. Width of Cross-Correlation Functions vs. Separation in Time.

In many cases, although the end of strand was out of focus, good sequences of the performance of the inhibitor were obtained. The melting and bubbling of inhibitors and the smoking and/or flaking of some inhibitors showed clearly. So, as a side effect, the studies show that copper-vapor laser illumination gives good information on inhibitor performance. Small adjustments were made in the scattering geometry to achieve as much shadowing by particles as possible. Not much could be done if the incoming laser beam did not strike the surface at an oblique angle. This would require either cutting strands with square ends or reconfiguring the window bomb. The angle at which the laser beam or camera was oriented with respect to the windows could not be moved by very much, due to the limited size of the ports and the increase in reflections if normal incidence was not used. If the strands were not cut at a 45° angle, the depth-of-field problem over most of the field-of-view would be accentuated.

CONCLUSIONS

The utility of copper-vapor laser illumination for high-resolution, high-speed cinemography of solid-propellant deflagration has been demonstrated. Movies can be made with a ratio of the field dimension to the smallest resolvable dimension which is greater than 500. These movies are unimpaired by flame brightness, motion blur, or laser speckle.

The performance of the experiment is critically dependent on the combined Modulation Transfer Function of the camera lens and film. Since the depth-of-field and resolution are coupled, high resolution exacts a penalty of a severely limited depth-of-field.

The use of white-light illumination prior to this program has placed severe constraints on the depth-of-field and field-of-view that can be obtained from such films at high resolution. The use of an intense pulsed laser for illumination relaxes these constraints. Consequently, it is now possible to survey an entire strand surface in detail. In this manner, meaningful statistical information can be obtained about particle behavior in the flame. In particular, analyses of interactions between particles and correlated behavior, if any, can be made.

At pressures below 500 psi, high-albedo features appear in a size range (50-200 microns) that do not occur in the original formulation. The widths of bright features vary with pressure, but not with propellant type. The features have been identified as highly reflecting areas on the sides of the large AP particles.

The concept of a photo-detector array has been demonstrated to achieve tight position control. Practical limitations are due to the number of diodes in the array and the quality of the motor drive and its controller. The main limitations of this circuit could best be alleviated by adding more elements to the array. Ultimate performance will be determined by the ability of the optical subsystem to overcome the lensing action of the propellant flame. Possibly this can be achieved with incoherent optics. The signal from the photodetector array gives an excellent record of the instantaneous local burning rate.

Correlator results demonstrate that simple optical systems can yield useful quantitative statistics on movies of random data fields. The existing correlator is difficult to align due to the requirement of an exact overlay between two frames, including successive frames in a movie, which never have exactly the same profile. It is more convenient to work with a high-contrast transparency than with a low-contrast one. Transparencies should be made under the same conditions and with the same exposure time for accurate results.

An inhibitor coating developed for solid propellants does not smoke or flake and can be tailored to match the burning rate of the propellant. The base for this inhibitor is a partially reacted phenolic polymer. This material completes its polymerization upon heating in the combustion process and subsequently chars. The monomer base comes in powder form. Experiments on 1/4-inch strands showed greatly superior performance compared to other materials commonly used in laboratory work.

A trade-off must often be made between detail in a film and visual quality. The MTF of a lens/film system falls off steadily with decreasing feature size. Low-contrast features are most severely affected by this fact, so that small-scale, low-contrast details tend to blur out. Large-grain film and a high-contrast developer result in a film with good visual clarity, while a fine-grain film and a soft developer give a more faithful representation of the object field. Similar considerations apply to reproductions, whether by motion picture projectors or enlargements of individual frames. The fine detail obtained in a soft picture leads to a blurred result in reproductions using standard commercial equipment.

Initial stereo feasibility studies on propellant combustion have been successfully completed. This demonstrates that stereo movies are possible, and problem areas that need improvement to make stereo movies practical have been identified. One such area is customized mirror mounts which need to be designed.

REFERENCES

1. Glick, R. L. and Becker, R. J., Recommended Experiments Related to Difluoramino Propellants, Report No. UDR-TR-81094, University of Dayton, Dayton, OH, August, 1981.
2. Mclean, W. B., Combustion of Solid Propellants and Low-Frequency Combustion Instability, NOTS TP 4244, 1967.
3. Sutton, E. S., From Polysulfides to CTPB Binders, A Major Transition in Solid Propellant Binder Chemistry, Paper presented to AIAA, No. 84-1236.
4. Flandro, G. A., A Simple Conceptual Model for the Nonlinear Transient Combustion of a Solid Rocket Propellant, Paper presented to AIAA, No. 82-1222.
5. Williams, F. A., Barrere, M., and Huanh, N. C., Fundamental Aspects of Solid Propellant Rockets, Technivision Services, Slough, England, 1969.
6. Culick, F. E. C., "Acoustic Oscillations in Solid Propellant Rocket Chambers." Astronautica Acta, Vol. 12, No. 2, P. 113, 1966.
7. Brown, R. S., Blackner, A. M., Willoughby, P. G., and Dunlap R., Coupling Between Velocity Oscillations and Solid Propellant Combustion, Paper No. 34 presented at AFOSR/RPL Chemical Rocket Research Meeting, Lancaster, CA, March, 1985.
8. Srivastava, R., Reaction Boundary Layer Model of Steady and Oscillatory Combustion of Solid Propellants, Paper presented to AIAA, No. 85-1110.
9. Levine, J. N. and Baum, J. D., Modeling of Nonlinear Combustion Instability in Solid Propellant Rocket Motors, Paper presented at nineteenth International Symposium on Combustion, 1982. Also published as--Baum, J. D. and Levin J. N., Nonlinear Combustion Intability in Solid Rocket Motors, Report No. UDR-TR-82-158, University of Dayton, Dayton, OH 1982.
10. Brown, R. S. and Waugh, R. C., Coupling Between Velocity Oscillations and Solid Propellant Combustion, Report No. CSD 2749-AR-1, United Technologies Chemical Systems Division.
11. Miller, R. R., Self-Extinguishment Propellant Development, AFRPL-TR-82-096, Air Force Rocket Propulsion laboratory, Edwards Air Force Base, CA, December 1982.

12. Strand, L. D. and McNamara, R. P., "A Variable-Frequency Driver-Microwave Transient Regression Rate Measurement System." in Experimental Diagnostics in Combustion of Solids, R. L. Boggs and B. T. Zinn, eds., American Institute of Aeronautics and Astronautics, 1978.
13. Strand, L. D., Investigation of Microwave Doppler Shift Measurement System of Solid Propellant Combustion Response Function, AFRPL-TR-83-085, Air Force Rocket Propulsion Laboratory, Edwards Air Force Base, CA, 1984.
14. Boggs, T. L., Derr, R. L., and Beckstead, M. W., "Surface Structure of Ammonium Perchlorate Composite Propellants." AIAA Journal, Vol. 8, No. 2, p. 370, 1969.
15. Hanzawa, M., A Theoretical Study on Depressurization Induced Extinction of Solid Propellant, Paper presented at AIAA, No. 76-635.
16. Merkle, C. L., Turk, S. L., and Summerfield, M., Extinguishment of Solid Propellants by Depressurization: Effects of Propellants Parameters, Paper presented to AIAA, No. 69-176.
17. Jensen, G. E., An Experimental Study of Solid Propellant Extinguishment by Rapid Depressurization, NASA Technical Report CR-66747, 1969.
18. Gony, A., Combustion Studies of Metallized Fuels for Solid Fuel Ramjets, Paper presented to AIAA, No. 85-1177.
19. Boggs, T. L. and Zinn, B. T., eds., Experimental Diagnostics in Combustion of Solids, American Institute of Aeronautics and Astronautics, 1978.
20. Boggs, T. L., Crump, J. E., Kraeutle, K. J. and Zurn, D. E., "Cinephotomicrography and Scanning Electron Microscopy as Used to Study Solid Propellant Combustion." in Experimental Diagnostics in Combustion of Solids, T. L. Boggs and B. T. Zinn, eds., American Institute of Aeronautics and Astronautics, 1978.
21. Laird, J. L., Luehrmann, P. F., and Becker, R. J., Application of a Copper-Vapor Laser to High-Speed, High-Resolution, Front-Lit Cinephotography of Solid Propellant Deflagration, Paper presented to AIAA, No. 85-1257.
22. Laird, J. L. and Becker, R. J., "A Novel Smokeless, Non-Flaking Solid Propellant Inhibitor." To be published in Journal of Propulsion and Power.

23. Andrews, C. L., Optics of the Electromagnetic Spectrum, Prentic-Hall Publishing Co., Englewood Cliffs, NJ, 1960.
24. Optics Guide, 3, Melles Griot, Irvine, CA, 1985.
25. Hect, E. and Zajac, A., Optics, Addison-Wesley Publishing Co., Reading, MA, 1979.
26. Becker, R. J. and Aulds, J. M., "Design and Performance of a Detector Array Servopositioner for Strand Experiments." Submitted to the Journal of Propulsion and Power.
27. Becker, R. J. and Laird, J. L., Optical Consideration in Obtaining a Statistical Data Base on Propellant Deflagration, Paper presented at JANNAF Combustion Meeting, Pasadena, CA, October 1985.
28. Edwards, T., Weaver, D. P., and Adams, R., "A High-Pressure Combustor for the Spectroscopic Study of Solid Propellant Combustion Chemistry." Submitted to Review of Scientific Instruments.
29. Culick, F. E. C., "Acoustic Oscillations in Solid Propellant Rocket Chambers." Astronautica Acta, Vol. 12, No. 2, p. 113, 1966.
30. Culick, F. E. C., "A Review of Calculations for Unsteady Burning of a Solid Propellant." AIAA, Vol. 12, No. 6, pp. 2241-54, 1968.
31. Cohn, N. S., Combustion Response Functions of Homogeneous Propellants, Paper AIAA-85-1114, presented at AIAA/SAE/ASME/ASEE 21st Joint Propulsion Conference, Monterey, CA, July 1985.
32. Wilson, J. R. and Micci, M. M., Direct Measurement of High-Frequency Solid Propellant Pressure-Coupled Responses, Paper presented to AIAA, No. 85-113.
33. Beckstead, M. W. and Culick, F. E. C., A Comparison of Analysis and Experiment for Solid Propellant Combustion Instability, Naval Weapons Center Technical Publication 4531, 1968.
34. Combustion Tailoring Criteria for Solid Propellants, AFRPL-TR-69-190, Lockheed Propulsion Co., 1969.
35. Osborn, J. R., "Evaluation of Solid Propellant Ballistic Properties." Combustion and Flame, Vol. 20, pp. 193-97, 1973.

36. Becker, R. J., Luehrmann, P. F., Laird, J. L., and Heinrichs, J. J., Application of a Pulsed Laser to Cinephotography of Deflagration over Extended Surfaces." Submitted to the Journal of Propulsion and Power.
37. Becker, R. J. and Al-Saffar, M. A., "A Simple Optical Correlator for the Quantitative Statistical Data Analysis of Photographs of Random Fields." Submitted to the Journal of Propulsion and Power.
38. Pratt, W. K., Digital Image Processing, John Wiley Publishing Co., New York, 1978.
39. Monanan, M. A. Bromley, K., and Bocker, R. P. "Incoherent Optical Correlations." Proc. IEEE, Vol. 65, p. 121, 1977.
40. Rhodes, W. T. and Sawchuk, A. A., "Incoherent Optical Processing." From Topics in Applied Physics, Vol. 48, Optical Information Processing Fundamentals, S. H. Lee, ed., Springer-Verlag Publishing Co., New York, 1981.
41. Goodman, J. W., Introduction to Fourier Optics, McGraw-Hill Publishing Co., New York, 1968.
42. Becker, R. J., Laird, J. L., and Heinrichs, J. J., "Front-Lit Stereo Cinephotography of Solid Propellant Combustion." Submitted to the Journal of Propulsion and Power.
43. Bevington, P. R., Data Reduction and Error Analysis for the Physical Sciences, McGraw-Hill Publishing Co., New York, 1969.

CREDITS

1 TECHNICAL JOURNAL ARTICLES--ACCEPTED FOR PUBLICATION

J. L. Laird and R. J. Becker, "A Novel Smokeless, Non-Flaking Solid Propellant Inhibitor," submitted to the Journal of Propulsion and Power.

2 TECHNICAL JOURNAL ARTICLES--SUBMITTED

R. J. Becker and J. M. Aulds, "A Diode-Array Servocontroller for Propellant Strand Experiments," submitted to the Journal of Propulsion and Power.

R. J. Becker and M. A. Al-Saffar, "A Simple Optical Correlator for the Quantitative Statistical Data Analysis of Photographs of Random Fields," submitted to the Journal of Propulsion and Power.

R. J. Becker, R. F. Luehrmann, J. L. Laird, and J. J. Heinrichs, "Application of a Pulsed Laser to Cinephotography of Deflagration Over Extended Surfaces," Submitted to the Journal of Propulsion and Power.

R. J. Becker, J. L. Laird, and J. J. Heinrichs, "Front-Lit, Stereo Cinephotography of Solid Propellant Combustion," submitted to the Journal of Propulsion and Power.

3 PRESENTATIONS

R. J. Becker, "Pulsed-Laser High-Speed Photography of Propellant Deflagration," AFOSR/AFRPL Contractors Meeting, Lancaster, CA, March 1984.

P. F. Luehrmann and R. J. Becker, "High-Resolution Cinephotography in a Flame Using a Copper-Vapor Laser," OS/APS Annual Fall Meeting, Cleveland State University, Cleveland, OH, October 1984.

P.F. Luehrmann and R. J. Becker, "Pulsed-Laser, High-Speed Photography of Rocket Propellant Deflagration," OSA Annual Meeting, San Diego, CA, November, 1984.

R. J. Becker, "Data Processing of Time-Dependent Multiplexed Signals from Stochastic Systems," Society for Applied Spectroscopy, Ohio Valley Section Poster Session, January, 1985.

R. J. Becker, "High-Speed Cinemicroscopy on Burning Surfaces," Seminar Presented at Miami University, Oxford, OH, February 1985.

M. A. Al-Saffar and R. J. Becker, "Statistical Analysis of Topographic Data Using an Optical Correlator," 11th Annual AIAA Mini-Symposium on Aerospace Science and Technology, W-PAFB, OH, March 19, 1985.

J. L. Laird, P. F. Luehrmann, and R. J. Becker, "High-Resolution Pulsed-Laser Photography of Solid Propellant Deflagration," 11th Annual AIAA Mini-Symposium on Aerospace Science and Technology, W-PAFB, OH, March 1985.

C. E. Orr and R. J. Becker, "Hilbert Transform Analysis of Solid-Propellant Response Functions," 11th Annual AIAA Mini-Symposium on Aerospace Science and Technology, W-PAFB, OH, March 1985.

R. J. Becker, P. F. Luehrmann, and J. L. Laird, "High-Resolution Movies of Propellant Deflagration," AFCSR/AFRPL Chemical Rocket Research Meeting, Lancaster, CA, March 1985.

J. L. Laird, J. J. Heinrichs, and R. J. Becker, "High-Speed Photography of Solid Propellant Deflagration," Ohio Section Meeting of the American Physical Society, Cincinnati, OH, April 1985.

J. L. Laird, P. F. Luehrmann, and R. J. Becker, "Application of a Copper-Vapor Laser to High-Speed, High-Resolution, Front-Lit Cinematography of Solid Propellant Deflagration," AIAA/SAE/ASME/ASEE 21st Joint Propulsion Conference, July, 1985, Monterey, CA, AIAA Paper No. 85-1257.

R. J. Becker and J. L. Laird, "Optical Considerations in Obtaining a Statistical Data Base on Propellant Deflagration," JANNAF Meeting on Combustion, Pasadena, CA, October 1985.

4 INVENTION DISCLOSURES

<u>Disclosure Number</u>	<u>Date of Disclosure</u>	<u>Title of Invention</u>	<u>Inventor(s)</u>
---	11-6-84	Chemical Inhibitor for Solid Propellants	Janet L. Laird Ival O. Salyer Roger J. Becker
006	5-14-85	Pulsed Synchronization Circuit	J. Michael Aulds
008	4-30-85	Optical Correlator for Analysis of Random Fields	Roger J. Becker Allan Buswell M. A. Al-Saffar

<u>Disclosure Number</u>	<u>Date of Disclosure</u>	<u>Title of Invention</u>	<u>Inventor(s)</u>
010	5-28-85	Strand Position Servo-controller	Roger J. Becker Andrew Piekutowski J. Michael Aulds
011	5-29-85	High-Resolution Cinephotographics System	Roger J. Becker J. Michael Aulds
013	5-28-85	Diode Array Detector for Proportional Drive Servocontrol	J. Michael Aulds Roger J. Becker